European Journal of Pharmaceutical Sciences 162 (2021) 105810

Contents lists available at ScienceDirect

European Journal of Pharmaceutical Sciences

journal homepage: www.elsevier.com/locate/ejps

An automated cocktail method for in vitro assessment of direct and time-dependent inhibition of nine major cytochrome P450 enzymes – application to establishing CYP2C8 inhibitor selectivity

Helinä Kahma [a,b,c,1], Laura Aurinsalo [a,b,1], Mikko Neuvonen [a,b], Jani Katajamäki [a,b], Marie-Noëlle Paludetto [a,b], Jenni Viinamäki [a], Terhi Launiainen [a], Anne M. Filppula [a,b], Aleksi Tornio [a,b,c,2], Mikko Niemi [a,b,c], Janne T. Backman [a,b,c,*]

[a] Department of Clinical Pharmacology, University of Helsinki, Helsinki, Finland
[b] Individualized Drug Therapy Research Program, Faculty of Medicine, University of Helsinki, Helsinki, Finland
[c] Department of Clinical Pharmacology, HUS Diagnostic Center, Helsinki University Hospital, Helsinki, Finland

ARTICLE INFO

Keywords:
Cytochrome P450
Substrate cocktail
Time-dependent inhibition
Drug metabolism
Metabolic interactions
Gemfibrozil 1-*O*-β-glucuronide

ABSTRACT

We developed an *in vitro* high-throughput cocktail assay with nine major drug-metabolizing CYP enzymes, optimized for screening of time-dependent inhibition. The method was applied to determine the selectivity of the time-dependent CYP2C8 inhibitors gemfibrozil 1-*O*-β-glucuronide and clopidogrel acyl-β-D-glucuronide. *In vitro* incubations with CYP selective probe substrates and pooled human liver microsomes were conducted in 96-well plates with automated liquid handler techniques and metabolite concentrations were measured with quantitative UHPLC-MS/MS analysis. After determination of inter-substrate interactions and K_m values for each reaction, probe substrates were divided into cocktails I (tacrine/CYP1A2, bupropion/CYP2B6, amodiaquine/CYP2C8, tolbutamide/CYP2C9 and midazolam/CYP3A4/5) and II (coumarin/CYP2A6, *S*-mephenytoin/CYP2C19, dextromethorphan/CYP2D6 and astemizole/CYP2J2). Time-dependent inhibitors (furafylline/CYP1A2, selegiline/CYP2A6, clopidogrel/CYP2B6, gemfibrozil 1-*O*-β-glucuronide/CYP2C8, tienilic acid/CYP2C9, ticlopidine/CYP2C19, paroxetine/CYP2D6 and ritonavir/CYP3A) and direct inhibitor (terfenadine/CYP2J2) showed similar inhibition with single substrate and cocktail methods. Established time-dependent inhibitors caused IC_{50} fold shifts ranging from 2.2 to 30 with the cocktail method. Under time-dependent inhibition conditions, gemfibrozil 1-*O*-β-glucuronide was a strong (>90% inhibition) and selective (<< 20% inhibition of other CYPs) inhibitor of CYP2C8 at concentrations ranging from 60 to 300 μM, while the selectivity of clopidogrel acyl-β-D-glucuronide was limited at concentrations above its IC_{80} for CYP2C8. The time-dependent IC_{50} values of these glucuronides for CYP2C8 were 8.1 and 38 μM, respectively. In conclusion, a reliable cocktail method including the nine most important drug-metabolizing CYP enzymes was developed, optimized and validated for detecting time-dependent inhibition. Moreover, gemfibrozil 1-*O*-β-glucuronide was established as a selective inhibitor of CYP2C8 for use as a diagnostic inhibitor in *in vitro* studies.

1. Introduction

Drug-drug interactions caused by inhibition of cytochrome P450 (CYP) enzymes are a common cause of adverse effects. One of the most hazardous and often overlooked mechanisms of CYP enzyme inhibition is time-dependent inhibition (TDI). TDI may be caused by several different mechanisms, including formation of reactive electrophiles, which inactivate enzymes by forming covalent bonds, or generation of tight bonds between the heme component of cytochrome P450 enzymes and drug metabolites (Silverman, 1995; Guengerich, 2003; Kalgutkar et al., 2007). After stopping treatment with this kind of inhibitors *in vivo*, synthesis of new enzymes gradually recovers enzyme function during

* Corresponding author at: Department of Clinical Pharmacology, University of Helsinki, Biomedicum 2C, Tukholmankatu 8 C, 00290 Helsinki, Finland.
E-mail address: janne.backman@helsinki.fi (J.T. Backman).
[1] These authors contributed equally.
[2] Current affiliation: Integrative Physiology and Pharmacology, Institute of Biomedicine, University of Turku, Turku, Finland; Unit of Clinical Pharmacology, Turku University Hospital, Turku, Finland.

https://doi.org/10.1016/j.ejps.2021.105810
Received 15 December 2020; Received in revised form 26 February 2021; Accepted 16 March 2021
Available online 19 March 2021

the following days or weeks (Tornio et al., 2008; Juřica and Žourková, 2013; Kaartinen et al., 2020). Compared to reversible direct inhibition, the effect of TDI thus has a substantially longer timescale. A demonstrative example of such a time-dependent inhibitor is the lipid lowering fibrate gemfibrozil. Initially, its drug interactions obtained worldwide attention, as it drastically increased the risk of rhabdomyolysis during cerivastatin treatment, which led to withdrawal of cerivastatin in 2001 (World Health Organization, 2001; Backman et al., 2002; Roca et al., 2002; Thompson et al., 2003; Tornio et al., 2017). The mechanism of this potentially fatal interaction was later found to be strong mechanism-based inhibition of CYP2C8 caused by its major glucuronide metabolite (Ogilvie et al., 2006). Consequently, gemfibrozil causes a time- and dose-dependent CYP2C8 inhibition that lasts a few days after gemfibrozil has been eliminated (Backman et al., 2009; Honkalammi et al., 2011a; Honkalammi et al., 2011b; Honkalammi et al., 2012).

Assessment of drug-drug interactions is essential in the development of a new drug. If potentially hazardous interactions are not detected in the preclinical phase, they can cause even life-threatening adverse effects to patients during clinical treatment. Investigating both direct and time-dependent inhibition of at least CYP1A2, CYP2B6, CYP2C8, CYP2C9, CYP2C19, CYP2D6 and CYP3A4 *in vitro* is recommended before proceeding to clinical trials (European Medicines Agency, 2012; U.S. Food and Drug Administration, 2020). Direct inhibition is studied through a short co-incubation of the investigated drug with HLM, NADPH and a marker substrate, whereas TDI assays require an additional preincubation step. Preincubating a test compound for 30 minutes with HLM and NADPH prior to addition of the probe substrate is a well-established method to investigate TDI, which is evidenced by a preincubation time- and NADPH-dependent increase of inhibitory potency (i.e. by a shift to a lower IC_{50} value upon preincubation). To improve the throughput of often time-consuming CYP inhibition screening during drug development, fluorescence, luminescence and radioactive assays using recombinant CYP enzymes have been widely used for evaluating inhibition of major CYP enzymes. However, these assays have several drawbacks, including lack of specific probes, poor *in vitro - in vivo* correlation and discrepancies between TDI data obtained using recombinant CYPs and human liver microsomes (HLMs) (Cohen et al., 2003; Parkinson et al., 2010; Kahma et al., 2019). An LC-MS-based substrate cocktail approach, in which multiple CYP activities are assessed in a single experiment in HLMs, provides more reliable results and can offer high throughput, especially when automated liquid handling is used. Various *in vitro* cocktail methods have been developed for assessment of drug-drug interactions (Spaggiari et al., 2014). Yet, a majority of them have been designed for detecting direct inhibition and only few methods have been validated and optimized for screening of TDI, usually lacking automation and often including only a limited selection of CYP enzymes (Atkinson et al., 2005; Mori et al., 2009; Spaggiari et al., 2014; Lee and Kim, 2013; Kozakai et al., 2014; Dahlinger et al., 2016; Chen et al., 2016).

Our aim was to establish an *in vitro* high-throughput cocktail method utilizing liquid-handling robotics, with optimized incubation conditions for detection of TDI of drug metabolizing CYP enzymes, including all seven enzymes recommended by FDA and EMA, and additionally CYP2A6 and CYP2J2, which are involved in the metabolism of a number of important drugs (Spracklin et al., 1996; Sadeque et al., 1997; Hashizume et al., 2002; Lee, et al., 2010; Karkhanis et al., 2017). Additionally, as there is only very limited knowledge on the inhibitory effects of clopidogrel acyl-β-D-glucuronide and gemfibrozil 1-O-β-glucuronide on CYP enzyme activities, apart from their time-dependent CYP2C8 inhibitory effect (Ogilvie et al., 2006; Floyd et al., 2012; Tornio et al., 2014), we used the method to assess their potential to cause direct or time-dependent inhibitory effects on all the nine CYP enzymes. Accordingly, we wanted to comprehensively document their usefulness as diagnostic CYP2C8 inhibitors.

2. Materials and methods

2.1. Materials

Pooled HLMs from 200 donors (XTreme 200 Mixed Gender) were purchased from XenoTech (Kansas City, KS, USA). Human recombinant CYP2C19 expressed in baculovirus infected insect cells with human cytochrome b5 (Supersomes) were purchased from Corning (Corning, NY, USA). Bovine serum albumin (BSA) was from Biowest (Nuaillé, France). Amodiaquine dihydrochloride, coumarin, dextromethorphan hydrobromide, (±)-omeprazole, 1-hydroxymidazolam, 1-hydroxymidazolam-d4, 6β-hydroxytestosterone, 6β-hydroxytestosterone-d3 and β-NADPH were from Sigma-Aldrich (St. Louis, MO, USA). Astemizole, astemizole-d3, bupropion hydrochloride, chlorzoxazone, dextrorphan tartrate, dextrorphan-d3 tartrate, diclofenac sodium, furafylline, hydroxybupropion, hydroxybupropion-d6, hydroxytolbutamide, hydroxytolbutamide-d9, *N*-desethylamodiaquine hydrochloride, *N*-desethylamodiaquine-d5, *O*-desmethylastemizole, ritonavir, *R*-omeprazole, selegiline hydrochloride, *S*-mephenytoin, *S*-(+)-clopidogrel hydrogen sulfate, tacrine hydrochloride, terfenadine, ticlopidine hydrochloride, tienilic acid, tolbutamide, 1-hydroxytacrine-d3, 4-hydroxydiclofenac, 4-hydroxydiclofenac-d4, 5-hydroxyomeprazole sodium, 5-hydroxyomeprazole-d3 sodium, 6-hydroxychlorzoxazone, 6-hydroxychlorzoxazone-d2, 7-hydroxycoumarin and 7-hydroxycoumarin-d5 were purchased from Toronto Research Chemicals (Toronto, ON, Canada). Gemfibrozil 1-*O*-β-glucuronide and 1-hydroxytacrine maleate were obtained from Santa Cruz Biotechnology (Dallas, TX, USA), clopidogrel acyl-β-D-glucuronide (contains 8.5% clopidogrel carboxylic acid, no clopidogrel detected) from Acanthus Research (Mississauga, ON, Canada), midazolam from Hoffmann-La Roche (Basel, Switzerland), *O*-desmethylastemizole-d4 from Medical Isotopes (Pelham, NH, USA), paroxetine hydrochloride from SynFine Research (Richmond Hill, ON, Canada), and testosterone from Fluka (Morris Plains, NJ, USA). Other solvents and reagents were of analytical grade.

2.2. Preliminary substrate testing

Probe substrate candidates for each CYP enzyme were chosen based on selectivity of the CYP-reaction, enzymatic turnover of the substrates and the risk of interactions with other CYPs in the cocktail incubation system. The following substrates were selected for preliminary testing: 5 μM tacrine (CYP1A2), 1 μM coumarin (CYP2A6), 100 μM bupropion (CYP2B6), 2 μM amodiaquine (CYP2C8), 10 μM paclitaxel (CYP2C8), 5 μM diclofenac (CYP2C9), 100 μM tolbutamide (CYP2C9), 20 μM racemic omeprazole (CYP2C19), 20 μM *R*-omeprazole (CYP2C19), 40 μM *S*-mephenytoin (CYP2C19), 5 μM dextromethorphan (CYP2D6), 50 μM chlorzoxazone (CYP2E1), 0.3 μM astemizole (CYP2J2), 2 μM midazolam (CYP3A4/5) and 40 μM testosterone (CYP3A4). The initial probe substrate concentrations were similar to their published K_m values.

Secondary selection of the substrates was based on solubility of the compounds in working solutions and aqueous buffer. Furthermore, the selectivity of CYP2C19-mediated omeprazole metabolism was tested using a preliminary cocktail consisting of racemic omeprazole or *R*-omeprazole, coumarin, dextromethorphan and astemizole. The IC_{50} of the CYP2C19-inhibitor ticlopidine was determined with and without a 30-minute preincubation of the inhibitor with HLMs (protein concentration 0.05 mg/mL) and NADPH (1 mM) followed by a 5-minute incubation with 20 μM racemic omeprazole/*R*-omeprazole alone or in cocktail. The experiments were otherwise conducted following the IC_{50} shift protocol described in section 2.6, with the exception that no BSA was added to the incubations. For *R*-omeprazole, IC_{50} values were also determined using human recombinant CYP2C19 (protein concentration 0.05 mg/mL) instead of HLMs.

Lastly, selected probe substrates were divided into two cocktails based on previously reported interactions between the substrates (Ren et al., 2013; Spaggiari et al., 2014; Dahlinger et al., 2016). Cocktail I

included 5 μM tacrine, 100 μM bupropion, 2 μM amodiaquine, 100 μM tolbutamide and 2 μM midazolam. Cocktail II included 1 μM coumarin, 40 μM *S*-mephenytoin, 5 μM dextromethorphan, 50 μM chlorzoxazone, 0.3 μM astemizole and 40 μM testosterone. Inter-substrate interactions in the cocktails were then evaluated by incubating each substrate with all other substrates from the same cocktail in a pairwise manner using incubation conditions described in section 2.3.

2.3. Final incubation conditions

After preliminary testing, the following substrates were selected for each CYP in the final cocktails: 5 μM tacrine for CYP1A2, 50 μM bupropion for CYP2B6, 2 μM amodiaquine for CYP2C8, 100 μM tolbutamide for CYP2C9 and 2 μM midazolam for CYP3A4/5 in cocktail I, and 1 μM coumarin for CYP2A6, 40 μM *S*-mephenytoin for CYP2C19, 5 μM dextromethorphan for CYP2D6 and 0.3 μM astemizole for CYP2J2 in cocktail II (Table 1). Incubations were carried out in at least triplicates in 96-well plates. The stock solutions of substrates were prepared in water or methanol. The substrates were diluted in 0.1 M sodium phosphate buffer (pH 7.4) with HLMs (0.05 mg/mL for cocktail I and 0.1 mg/mL for cocktail II). A small amount of bovine serum albumin (BSA) (0.5% w/v) was added to cocktail II incubation mixture to enhance CYP2C19 activity, as previously demonstrated by Peng et al. (2015), and the incubation mixture was prewarmed on a heated shaker (350 rpm, 37°C; Eppendorf ThermoMixer, Hamburg, Germany) for 3 minutes. A 5-minute incubation was initiated by the addition of NADPH (1 mM). Incubations were terminated by mixing one part sample with three parts ice cold methanol containing internal standards for each quantified metabolite (Table 2). To precipitate the proteins, the samples were kept at 4°C for at least 30 minutes before centrifugal filtration (1800 g, 15 minutes) through Strata Impact protein precipitation filter plates (Phenomenex, Torrance, CA, USA). The filtered samples were evaporated to dryness using a GeneVac centrifugal evaporator (Thermo Fisher Scientific, Waltham, MA, USA) and resuspended in 40 μL of 20% methanol for UHPLC-MS/MS analysis.

2.4. Linearity of metabolite formation

The linear range of metabolite formation was evaluated by incubating each substrate cocktail (Table 1) for 2.5, 5, 10, 15 or 30 minutes using a protein concentration of 0.05 mg/mL for cocktail I and 0.1 mg/mL for cocktail II. The effect of protein concentration was evaluated by incubating the substrate cocktails with three different protein concentrations (0.025 mg/mL, 0.05 mg/mL and 0.1 mg/mL for cocktail I and 0.05 mg/mL, 0.1 mg/mL and 0.2 mg/mL for cocktail II) for 5 minutes as described in section 2.3. For cocktail II, linearity was studied with and without BSA (0.5% w/v).

2.5. Determination of kinetic constants

Kinetic analysis of the final probe reactions was conducted by incubating each CYP substrate separately using 8-10 different substrate concentrations. The incubations followed the protocol described in section 2.3, with the exception of a shorter 2-minute incubation time used for amodiaquine, astemizole, coumarin and midazolam to avoid extensive depletion with the lowest concentrations of these high-turnover substrates. The kinetic data were analyzed with the following models using SigmaPlot (version 14.0; Systat Software, San Jose, CA, USA):

Michaelis-Menten

$$v = \frac{V_{max}\,[S]}{K_m + [S]} \quad (1)$$

where v is the initial velocity of the reaction, V_{max} is the maximal reaction velocity, [S] is the substrate concentration, and K_m is the Michaelis-Menten constant.

Substrate inhibition

$$v = \frac{V_{max}}{1 + \frac{K_m}{[S]} + \frac{[S]}{K_i}} \quad (2)$$

where K_i is the dissociation constant for the inhibitory substrate-enzyme-substrate complex.

Allosteric sigmoidal (Hill)

$$v = \frac{V_{max}[S]^n}{K_m^n + [S]^n} \quad (3)$$

where n is the Hill coefficient.

Two enzymes

$$v = \frac{V_{max1}[S]}{K_{m1} + [S]} + \frac{V_{max2}[S]}{K_{m2} + [S]} \quad (4)$$

The selection of the best model for each probe reaction was based on the Akaike information criterion, R^2 values, 95% confidence intervals (CI), and a visual examination of Michaelis-Menten and Eadie-Hofstee plots.

2.6. Automated IC_{50} shift assay

The final substrate cocktails were validated with a fully automated IC_{50} shift assay using well-characterized time-dependent or direct

Table 1
Probe substrates, CYP-specific model reactions, incubation concentrations of the substrates and K_m and V_{max} values expressed as mean (± standard error) of a single experiment run in triplicate.

	CYP	Substrate	Probe reaction	Incubation concentration *(μM)*	K_m *(μM)*	V_{max} *(pmol/min/mg)*	K_m, Literature *(μM)*
Cocktail I							
	1A2	Tacrine	1-Hydroxylation	5	7.1 (±2.1) (K_{m1}) 380 (±360) (K_{m2})	82 (±16) (V_{max1}) 360 (±210) (V_{max2})	16
	2B6	Bupropion	Hydroxylation	50	115 (±3.2)	145 (±1.3)	21-150
	2C8	Amodiaquine	*N*-Deethylation	2	2.2 (±0.14)	1380 (±26)	1.6-3.0
	2C9	Tolbutamide	4-Hydroxylation	100	241 (±18)	194 (±5.4)	93-440
	3A4	Midazolam	1'-Hydroxylation	2	2.6 (±0.22)	1250 (±31)	0.89-8.8
Cocktail II							
	2A6	Coumarin	7-Hydroxylation	1	0.8 (±0.066)	512 (±11)	0.84-5.6
	2C19	*S*-mephenytoin	4'-Hydroxylation	40	12 (±0.75)	41 (±0.66)	20-86
	2D6	Dextromethorphan	*O*-Demethylation	5	3.2 (±0.17)	206 (±3.0)	3.2-19.9
	2J2	Astemizole	*O*-Demethylation	0.3	0.8 (±0.044)	364 (±6.3)	0.1-26*

Literature K_m values were obtained from the University Washington Drug Interaction Database (DIDB; https://www.druginteractionsolutions.org [Accessed: 03-18-2020]), and are based on studies with pooled HLMs, except for those with *, which are from studies with recombinant enzymes. Literature K_m values reported in the table are determined without BSA.

Table 2
Mass spectrometry parameters for the quantified analytes in the UHPLC-MS/MS methods.

CYP	CYP-specific metabolite Internal standard	MRM transition *(m/z)*	ESI +/-	Q1 Pre-bias *(V)*	CE *(eV)*	Q3 Pre-bias *(V)*	Dwell time *(ms)*	LLOQ *(nM)*	Standard curve range ($R^2 > 0.99$) *(nM)*
Cocktail I									
1A2	1-hydroxytacrine	215.2 > 171.1	+	-24	-17	-21	10	1.0	1.0 – 100.0
	1-hydroxytacrine-d3	218.2 > 200.0	+	-24	-17	-21	10		
2B6	Hydroxybupropion	256.2 > 238.0	+	-28	-13	-26	10	0.3	0.3 – 50.0
	Hydroxybupropion-d6	262.2 > 244.0	+	-28	-13	-26	10		
2C8	*N*-desethylamodiaquine	328.3 > 283.1	+	-16	-20	-20	10	10.0	10.0 – 1000.0
	N-desethylamodiaquine-d5	333.3 > 283.1	+	-16	-20	-20	10		
2C9	4-hydroxytolbutamide	285.3 > 186.1	-	27	18	18	10	1.0	1.0 – 100.0
	4-hydroxytolbutamide-d9	294.2 > 186.0	-	27	18	18	10		
3A4	1'-hydroxymidazolam	342.1 > 323.9	+	-17	-20	-16	10	2.0	2.0 – 1000.0
	1'-hydroxymidazolam-d4	346.1 > 327.9	+	-17	-20	-16	10		
Cocktail II									
2A6	7-hydroxycoumarin	161.3 > 76.9	-	15	27	29	20	7.5	7.5 – 750.0
	7-hydroxycoumarin-d5	166.1 > 109.9	-	15	27	29	20		
2C19	*S*-4'-hydroxymephenytoin	235.2 > 150.1	+	-22	-17	-28	20	0.75	0.75 – 75.0
	4'-hydroxymephenytoin-d3	238.2 > 150.1	+	-22	-17	-28	20		
2D6	Dextrorphan	258.1 > 157.0	+	-13	-41	-16	20	0.5	0.5 – 250.0
	Dextrorphan-d3	261.1 > 157.0	+	-13	-41	-16	20		
2J2	*O*-desmethylastemizole	445.3 > 121.2	+	-21	-37	-25	20	1.5	1.5 – 250.0
	O-desmethylastemizole-d4	449.3 > 125.2	+	-21	-37	-25	20		

CE, collision energy; ESI, electrospray ionization; MRM, multiple reaction monitoring; Q1, quadrupole 1; Q3, quadrupole 3

inhibitors for each CYP enzyme (Figure 1). Time dependence of the inhibition was assessed using both the single substrates and the substrate cocktails. All dilutions and experiments were performed using a Tecan Freedom EVO 150 automated liquid handler, controlled using Freedom EVOware software (Tecan Group, Männedorf, Switzerland). The assay was designed for an IC_{50} shift experiment for 1-2 inhibitors at seven different concentrations with solvent controls. The reference inhibitor concentrations were chosen so that the highest concentrations would exceed the expected direct inhibition IC_{50} by at least an order of magnitude. The Tecan platform layout included racks for reagent reservoirs, a Tecan Te-Shake heated orbital shaker with a rack for a 96-well incubation plate, and an EcoTherm chilling dry bath (Torrey Pines Scientific, Carlsbad, CA, USA) with two 96-well plate racks, one for a reagent plate and one for a sample plate. Sample plates were covered with pierceable films (4titude, Wotton, UK) to prevent solvent evaporation during incubations. The working solutions of single substrates and the substrate cocktails were prepared in 80% methanol. The working solutions of the inhibitors were prepared in methanol, water or DMSO: methanol 2:3 (v/v), depending on inhibitor solubility. The final methanol and DMSO concentrations in the incubations were no more than 0.9% or 0.2%, respectively.

The direct inhibition and TDI incubations were performed simultaneously on a 96-well plate by timed pipetting of the reagents one column at a time. In TDI incubations, aliquots (1 μL) of the inhibitor or solvent control solutions were added in wells containing 0.1 M sodium phosphate buffer (pH 7.4). The plate was then moved onto the heated shaker and HLMs (10 μL, 0.05 or 0.1 mg/mL in final cocktail I and II incubations, respectively) were added in the wells. Thereafter, a 30-minute preincubation at 37 ℃ (550 rpm) was initiated by the addition of NADPH (10 μL, 1 mM in the final incubation). For cocktail II, a low concentration of BSA (10 μL, 0.5% w/v in the final incubation) was added to the incubation mixture 27 minutes after the start of the preincubation to increase enzyme activities in the final incubations (Peng et al., 2015). The final incubations to measure CYP activities were initiated by adding an aliquot (1 μL) of the substrate cocktails or single substrate solutions to give a final volume of 200 μL. After a 5-minute incubation on the heated shaker, 30 μL-samples were transferred to quenching wells in a cold (4°C) dry bath containing 90 μL of internal standard solution in methanol. The direct inhibition incubations followed the protocol described in section 2.3 with a 3-minute warm-up of HLMs, substrates and the inhibitor in buffer and a 5-minute incubation using the same pipetting volumes as in TDI incubations. The setup and other details of the automated assay will be made freely available and kept updated on the Zenodo open-access data repository (DOI: 10.5281/zenodo.4554651).

2.7. Determination of IC_{50} values

The enzyme activities with inhibitors were compared with identical control samples without inhibitors (solvent controls) and the IC_{50} values for the model inhibitors were calculated by nonlinear regression analysis using GraphPad Prism (version 7.04; GraphPad Software, La Jolla, CA, USA). The difference between IC_{50} values from direct and time-dependent inhibition experiments was compared, and the fold shift value was calculated by dividing the IC_{50} value obtained without preincubation by the IC_{50} value with preincubation.

2.8. Selectivity of TDI by clopidogrel acyl-β-D-glucuronide and gemfibrozil 1-O-β-glucuronide

The selectivity of time-dependent inhibition of CYP2C8 caused by the acyl glucuronides of clopidogrel and gemfibrozil was studied by conducting IC_{50} shift experiments with both substrate cocktails separately as described in sections 2.3 and 2.6. The inhibitor concentrations ranged from 96 nM to 1.5 mM in order to comprehensively evaluate their usefulness as *in vitro* diagnostic inhibitors.

2.9. UHPLC-MS/MS analysis

The quantitative analysis of the probe metabolites from 9 CYP-catalyzed reactions was performed using a Shimadzu Nexera X2 ultra-high-performance liquid chromatography system coupled to a Shimadzu LCMS-8050 triple quadrupole mass spectrometer (UHPLC-MS/MS) (Shimadzu, Kyoto, Japan). Analyte separation was performed with a Luna Omega Polar C18 column (100 × 2.1 mm internal diameter (i.d.), 1.6 μm particle size) (Phenomenex, Torrance, CA, USA) at a flow rate of 0.3 mL/min and column temperature of 40 °C. The autosampler temperature was set at 6 °C. The mobile phases consisted of 0.05% formic acid in water (A) and 0.05% formic acid in acetonitrile (B). The following gradient was used for Cocktail I samples: 0-1 min, B 10%; 1-3.5 min, B 10-27%; 3.5-5.5 min, B 27-90%; 5.5-7 min, B 90%; 7-7.1 min, B 90-10%; 7.1-15 min, B 10%. Cocktail II samples were

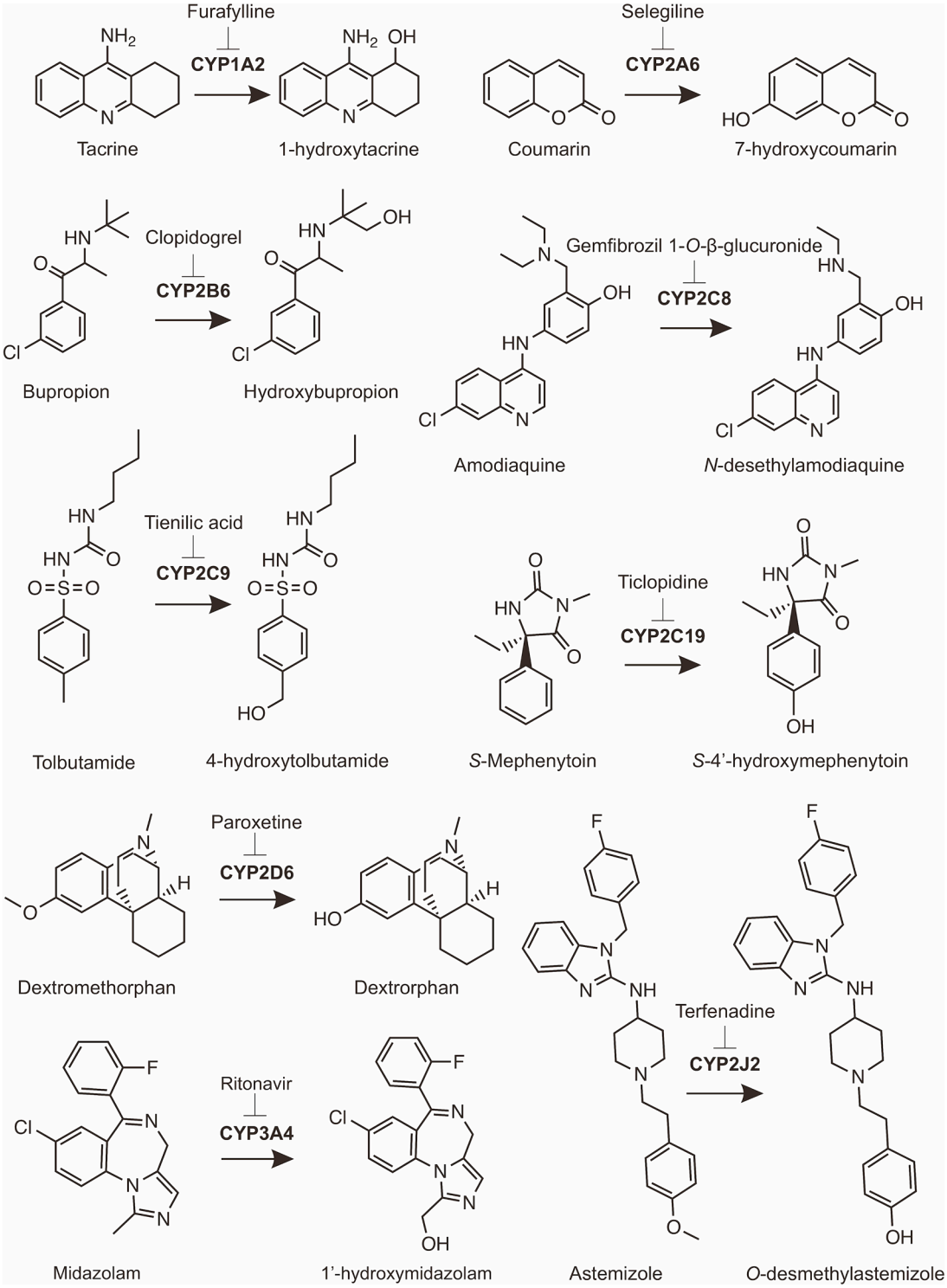

Fig. 1. Chemical structures of the probe substrates and their CYP-selective reactions. Reference inhibitors used in the validation process are indicated above each arrow.

separated using the following gradient: 0-0.5 min, B 10%; 0.5-5 min, B 10-30%; 5-6 min, B 30-70%; 6-6.1 min, B 70-95%; 6.1-8 min, B 95%; 8-8.1 min, B 95-10%; 8.1-15 min, B 10%. The injection volumes were 3 μL and 5 μL for Cocktail I and II samples, respectively. Mass spectra were acquired using electrospray ionization in both positive and negative ion mode. The following source-dependent parameter values were used: interface temperature 300 °C, desolvation line temperature 250 °C, heat block temperature 400 °C, nebulizing gas flow 3 L/min, heating gas flow 15 L/min and drying gas flow 10 L/min. The selected reaction monitoring transitions for each analyte, along with other analyte-related MS-parameters, standard curve ranges and lower limits of quantitation (LLOQ) are listed in Table 2. Data acquisition and treatment was performed using LabSolutions LCMS software (version 5.91; Shimadzu, Kyoto, Japan).

3. Results

3.1. Analytical method development

The optimal LC/MS precursor-product ion pairs were acquired using the pure reference compounds of each metabolite and their respective internal standards (Table 2). The negative ionization mode was selected for 4-hydroxytolbutamide, 7-hydroxycoumarin and their internal standards due to high intensity and low background noise, while the positive ionization mode was optimal for all other analytes. Chromatographic separation of the cocktail compounds was tested on three different analytical columns: Kinetex XB-C18 (50 × 2.1 mm i.d., 2.6 μm particle size, Phenomenex), Kinetex Hilic (50 × 2.1 mm i.d., 2.6 μm particle size, Phenomenex), and Luna Polar C18 (Phenomenex). Of these, the Luna Polar C18 column produced the best peak shape and resolution for the early eluting metabolites together with a complete separation of more lipophilic parent drugs. To avoid analytical interferences caused by metabolite-metabolite, metabolite-substrate and substrate-substrate co-elutions, baseline chromatographic separation of the analytes was optimized by using acetonitrile and 0.05% formic acid using different gradients for each cocktail as described in section 2.9.

The performance of the analytical methods was assessed, and calibration curves with at least six points ($R^2 > 0.99$) were constructed for the metabolites with a linear fit, except for 7-hydroxycoumarin and dextrorphan, which required a quadratic fit (Table 2 and Supplementary Table S1). The relative standard deviation (RSD) of the lower limits of quantitation (LLOQs) was below 20% for all analytes. No interference was observed for any of the analytes in blank samples (incubation matrix without metabolites, inhibitors or internal standards) or zero samples (blank sample including each inhibitor individually and internal standards). The intra- and inter-day accuracy and precision were within 15% for all analytes (Supplementary Table S1).

3.2. Selection of probe substrates and inter-substrate interactions

A number of probe substrates were rejected from the final cocktails based on the following reasons: poor solubility in aqueous solutions (paclitaxel), interactions with other substrates (chlorzoxazone and testosterone), precipitation when mixed with amodiaquine in working solutions (diclofenac) and lack of selectivity (racemic omeprazole and *R*-omeprazole). In preliminary TDI experiments, only 44% and 43% inhibition of CYP2C19 activity could be reached after a 30-minute preincubation with the potent CYP2C19 inhibitor ticlopidine (500 μM) using racemic omeprazole and *R*-omeprazole as the CYP2C19 substrate, respectively (Supplementary Figure S1). When using human recombinant CYP2C19 and *R*-omeprazole as the substrate, CYP2C19 activity was inhibited by 98% after a 30-minute preincubation with 500 μM ticlopidine.

In pairwise incubations of each substrate with all other substrates from the same cocktail, chlorzoxazone significantly inhibited CYP2A6-mediated coumarin 7-hydroxylation (38% inhibition), which was included in cocktail II (Figure 2). In further tests with cocktail I

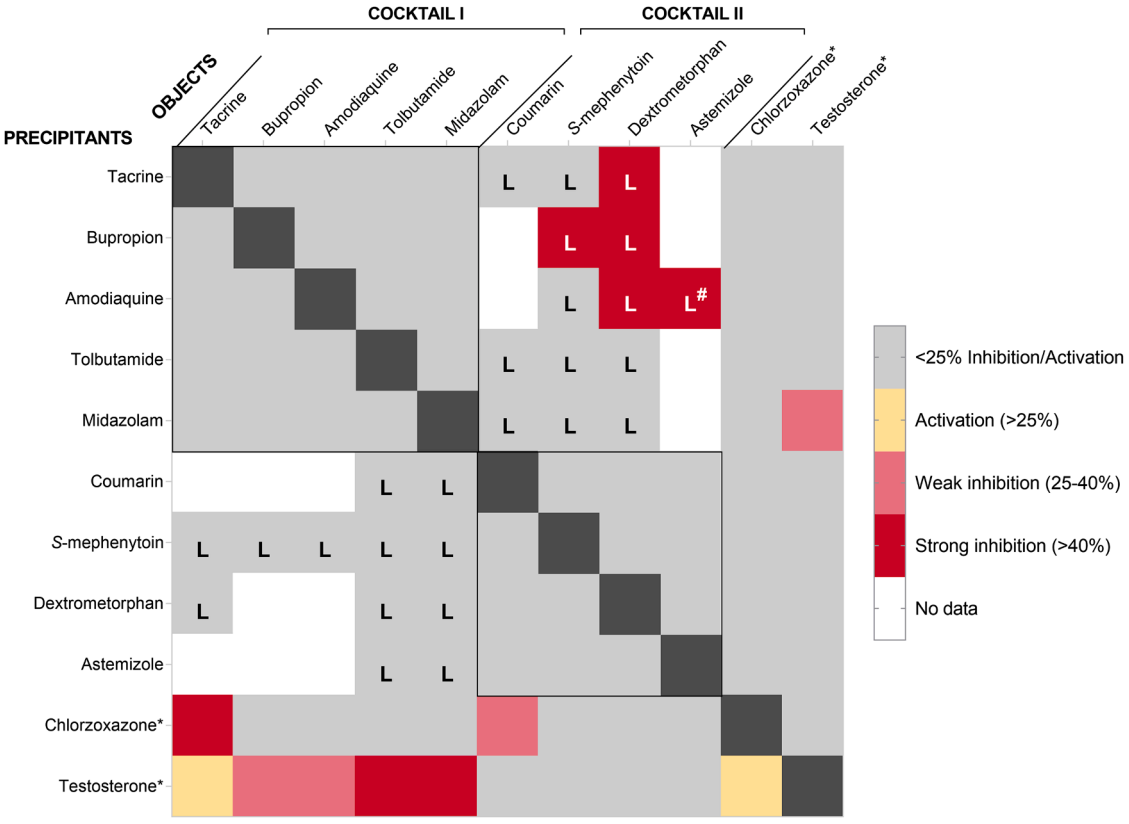

Fig. 2. One-to-one interactions between the probe substrates for CYP1A2 (5 μM tacrine), CYP2A6 (1 μM coumarin), CYP2B6 (50 μM bupropion), CYP2C8 (2 μM amodiaquine), CYP2C9 (100 μM tolbutamide), CYP2C19 (40 μM *S*-mephenytoin), CYP2D6 (5 μM dextromethorphan), CYP2E1 (50 μM chlorzoxazone), CYP2J2 (0.3 μM astemizole) and CYP3A4 (2 μM midazolam and 40 μM testosterone). CYP inhibition and activation are expressed as the percentage of CYP activity inhibited or activated compared to solvent controls without inhibitor (mean ± S.D. of a single experiment run in triplicate). Each of the probe substrates was tested as a precipitant (horizontal rows) to investigate their influence on the metabolism of the other probe substrates (objects, vertical columns). The degree of inhibition/activation is shown with the different colors. The final two cocktails are indicated with the black line around the respective rows and columns. L, Literature data obtained from the University of Washington Drug Interaction Database (DIDB; https://www.druginteractionsolutions.org [Accessed 5-15-2020]) is presented in cases where no in-house data was produced. #, Data obtained with recombinant enzymes.
*, Chlorzoxazone and testosterone were rejected from the final cocktails.

substrates, chlorzoxazone markedly inhibited CYP1A2-mediated tacrine 1-hydroxylation (50% inhibition) (Figure 2). Testosterone caused several interactions involving both cocktails, including significant activation of CYP1A2 (85% activation) and CYP2E1 (65% activation), and inhibition of CYP2B6 (26% inhibition), CYP2C8 (39% inhibition), CYP2C9 (44% inhibition) and the CYP3A4/5-mediated midazolam 1'-hydroxylation (43% inhibition) and slight inhibition of the low-turnover CYP2C19 substrate *S*-mephenytoin (12% inhibition). Based on the interaction potential in both cocktails, chlorzoxazone and testosterone were rejected from the methods. Of the other substrates, 100 μM bupropion inhibited CYP3A4/5-mediated midazolam 1'-hydroxylation by about 30%. Therefore, bupropion concentration was decreased to 50 μM, which did not significantly inhibit CYP3A4/5 activity (Figure 2). As the one-to-one interactions between the remaining substrates were minimal, no other modifications were made. In the final two cocktails, the CYP activities of the probe reactions were similar in the cocktail and single substrate experiments (Table 3), and the inhibitory effect of the full cocktail did not exceed 25% for any CYP.

3.3. Optimization of incubation conditions

Metabolite production was linear for more than five minutes for all probe reactions in final incubation conditions, except for midazolam, where the reaction rate started to decline from five minutes onwards (Supplementary Figure S2). Therefore, five minutes was chosen as the final incubation time. All reactions showed linear metabolism in a protein concentration range of 0.025-0.1 mg/mL for cocktail I and 0.05-0.2 mg/mL for cocktail II (data not shown). To produce enough 4'-hydroxymephenytoin for its reliable quantitation in case of strong CYP2C19 inhibition, a 0.1 mg/mL protein concentration was chosen for cocktail II, while 0.05 mg/mL was used in cocktail I. With the addition of 0.5% (w/v) BSA, the rate of *S*-mephenytoin 4'-hydroxylation was sufficiently accelerated to ensure reliable analytics and yet remained linear (Supplementary Figures S2 and S3).

3.4. Enzyme kinetic study

Because of the wide range of published K_m values and lack of enzyme kinetic data in pooled HLMs, we determined the K_m and V_{max} values for all the substrates (Table 1). With the exception of tacrine metabolism, all other CYP-specific reactions followed hyperbolic Michaelis-Menten kinetics (Figure 3). Tacrine 1-hydroxylation displayed biphasic kinetics, and the best fit for the reaction was obtained with the two-enzyme model.

Table 3
Metabolite formation rates in single substrate incubations compared to the cocktails and the respective CYP activities in the cocktails compared to control samples. All values are expressed as means of single experiments run in quadruplicates.

	CYP	Metabolite formation rate ± SD (*pmol/min/mg*)		CYP activity in cocktail as % of single substrate activity
		Single substrate	Cocktail	
Cocktail I				
	1A2	49 ± 1	48 ± 1	98%
	2B6	47 ± 1	46 ± 1	97%
	2C8	669 ± 12	563 ± 8	84%
	2C9	43 ± 7	39 ± 3	92%
	3A4	1196 ± 50	910 ± 21	76%
Cocktail II				
	2A6	314 ± 4	284 ± 9	90%
	2C19	33 ± 2	31 ± 0	93%
	2D6	110 ± 1	120 ± 2	110%
	2J2	100 ± 9	107 ± 5	108%

3.5. Validation of the experimental system

Reference inhibitors were used to assess our methods' ability to detect TDI (Table 4). As there is no well-established time-dependent inhibitor for CYP2J2, we used terfenadine as a direct CYP2J2 inhibitor. Expected results were obtained with all inhibitors, including terfenadine, and the IC_{50} values for each target CYP enzyme were almost identical with the single substrate method and the cocktail method (Table 4, Figure 4). Additionally, substantial IC_{50} shifts were observed for each time-dependent CYP inhibitor, proving that our cocktails sensitively detected TDI (Table 4).

As all reference inhibitors were tested with the cocktail setup, we also obtained data on both direct and time-dependent effects of the reference inhibitors on other CYP enzymes in the tested cocktail. Furafylline (50 μM) and clopidogrel (1 μM) did not cause more than 20% inhibition of any enzyme other than CYP1A2 and CYP2B6, respectively, in cocktail I (Figure 5). With the CYP2C9 inhibitor tienilic acid (600 μM), 68% direct inhibition of CYP2C8 was observed, while the IC_{50} was not reached for CYP1A2, CYP2B6 and CYP3A4/5. Ritonavir was a highly selective CYP3A4/5 inhibitor with concentrations up to 0.1 μM, as all other reactions were inhibited by less than 15%. In cocktail II, the CYP2A6 inhibitor selegiline (500 μM) inhibited CYP2C19, CYP2D6 and CYP2J2 by 96%, 89% and 55%, respectively. The CYP2C19 inhibitor ticlopidine (250 μM) showed weak TDI of CYP2A6, reaching 54% and 37% inhibition with and without preincubation, respectively. Additionally, 91% direct inhibition of CYP2D6 was detected. A moderate 15 μM concentration of the CYP2D6 inhibitor paroxetine caused 66% inhibition of CYP2J2 with preincubation and 50% inhibition without preincubation, suggesting TDI of CYP2J2. CYP2A6 and CYP2C19 were inhibited by less than 35%. The CYP2J2 inhibitor terfenadine (200 μM) inhibited CYP2A6, CYP2C19 and CYP2D6 by 57%, 90% and 99%, respectively. A more comprehensive assessment of the selectivity of the inhibition caused by clopidogrel and gemfibrozil glucuronides was performed in both cocktails.

3.6. Selectivity of TDI of CYP2C8 by clopidogrel acyl-β-D-glucuronide and gemfibrozil 1-O-β-glucuronide

Clopidogrel acyl-β-D-glucuronide inhibited CYP2C8 with almost identical IC_{50} values (37-38 μM) after preincubation with single substrate and cocktail methods (Table 4), and the IC_{50}-shift with the cocktail was 2.4-fold. The IC_{50} values for all other CYP enzymes were at least 10 times higher, i.e., above 300 μM (Figure 6). With 1500 μM clopidogrel acyl-β-D-glucuronide, only 20% of CYP2B6 and CYP2C9 activities and 30% of CYP2C19 activity remained with and without preincubation, while at least 50% of control activity was remaining for all other CYP enzymes. Gemfibrozil 1-*O*-β-glucuronide inhibited CYP2C8 with an IC_{50} of 8-10 μM after preincubation (Table 4), and the IC_{50}-shift was 15-fold in the cocktail. For all other CYP enzymes, only minimal inhibition was observed at 300 μM gemfibrozil 1-*O*-β-glucuronide (Figure 6). At the highest 1500 μM concentration, CYP2B6 was inhibited by approximately 70%, while other inhibitory effects were below 50%.

4. Discussion

To date, only few cocktail methods have been published for screening TDI of CYP enzymes, and most of them do not cover the recommended minimum of enzymes to test for CYP inhibition nor have optimal preincubation and incubation conditions for detection of TDI (Atkinson et al., 2005; Mori et al., 2009; Lee, and Kim, 2013; Kozakai et al., 2014; Dahlinger et al., 2016; Chen et al., 2016). Substrate interaction data is lacking in most of the previous TDI cocktail methods although there is a high risk for interactions particularly when more than five substrates are included in the same cocktail. In addition, none of the published cocktail methods can be used to evaluate TDI of the

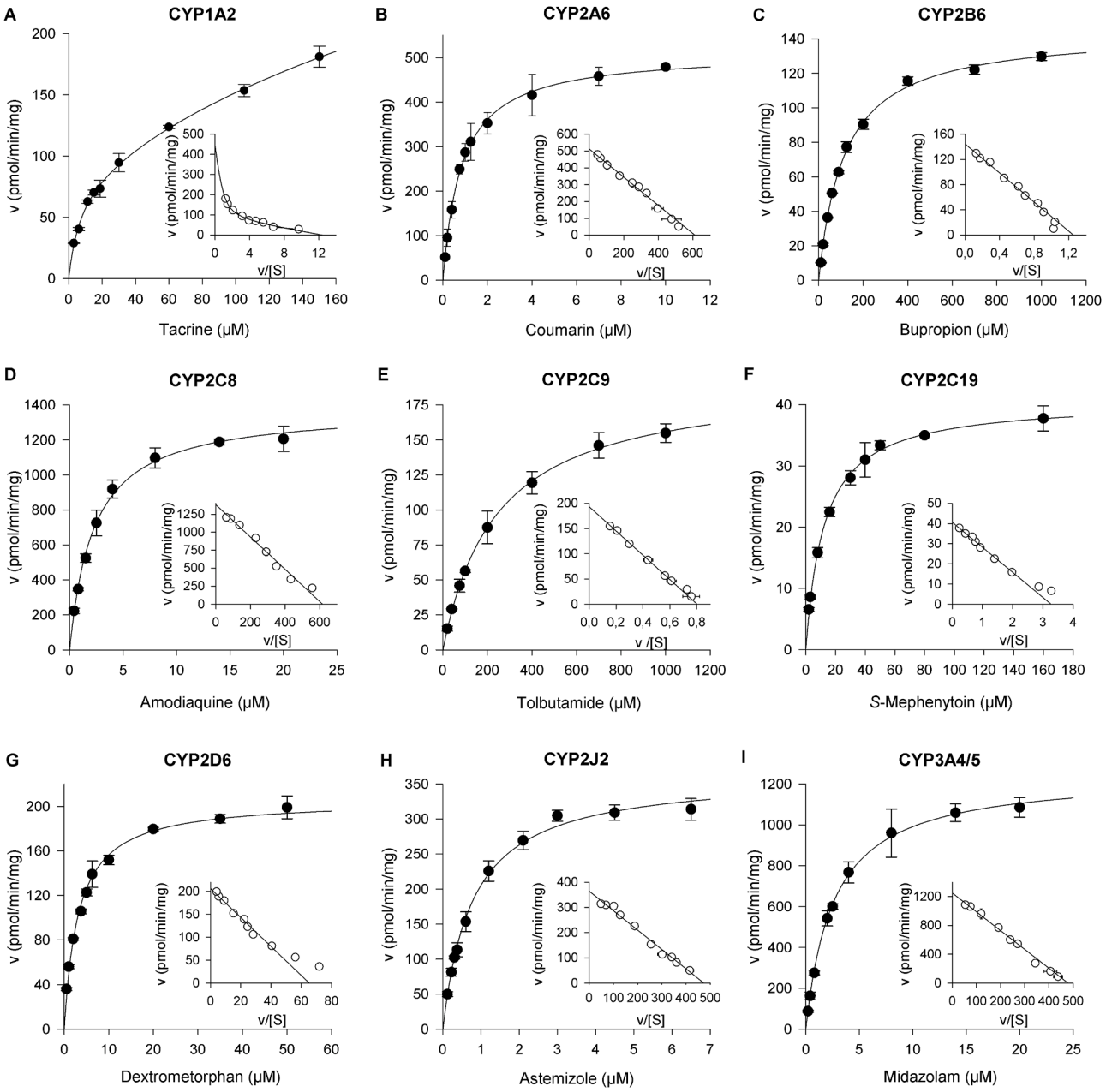

Fig. 3. Enzyme kinetics of tacrine 1-hydroxylation (A), coumarin 7-hydroxylation (B), bupropion hydroxylation (C), amodiaquine *N*-deethylation (D), tolbutamide 4-hydroxylation (E), *S*-mephenytoin 4'-hydroxylation (F), dextromethorphan *O*-demethylation (G), astemizole *O*-demethylation (H) and midazolam 1'-hydroxylation (I) in HLMs. Eadie–Hofstee plots are shown as insets. Each point represents the mean ± S.D. of a single experiment run in triplicate.

Table 4
IC_{50} values for the reference inhibitors with and without preincubation and the respective IC_{50} fold shifts. All values are expressed as means of single experiments run in triplicates.

Inhibitor	CYP	Substrate	IC_{50} Time-dependent inhibition		IC_{50} Direct inhibition	IC_{50} fold shift
			Single substrate (μM)	Cocktail (μM)	Cocktail (μM)	Cocktail
Furafylline	1A2	Tacrine	0.18	0.20	5.9	30
Selegiline	2A6	Coumarin	22	25	370	15
Clopidogrel	2B6	Bupropion	0.0047	0.0056	0.021	3.8
Clopidogrel acyl-β-D-glucuronide	2C8	Amodiaquine	38	37	89	2.4
Gemfibrozil 1-*O*-β -glucuronide	2C8	Amodiaquine	8.1	9.6	140	15
Tienilic acid	2C9	Tolbutamide	0.97	0.63	4.1	6.6
Ticlopidine	2C19	*S*-mephenytoin	0.64	1.0	3.3	3.2
Paroxetine	2D6	Dextromethorphan	0.027	0.029	0.71	24
Terfenadine	2J2	Astemizole	5.3	7.2	6.1	0.8
Ritonavir	3A4	Midazolam	0.0046	0.0040	0.0086	2.2

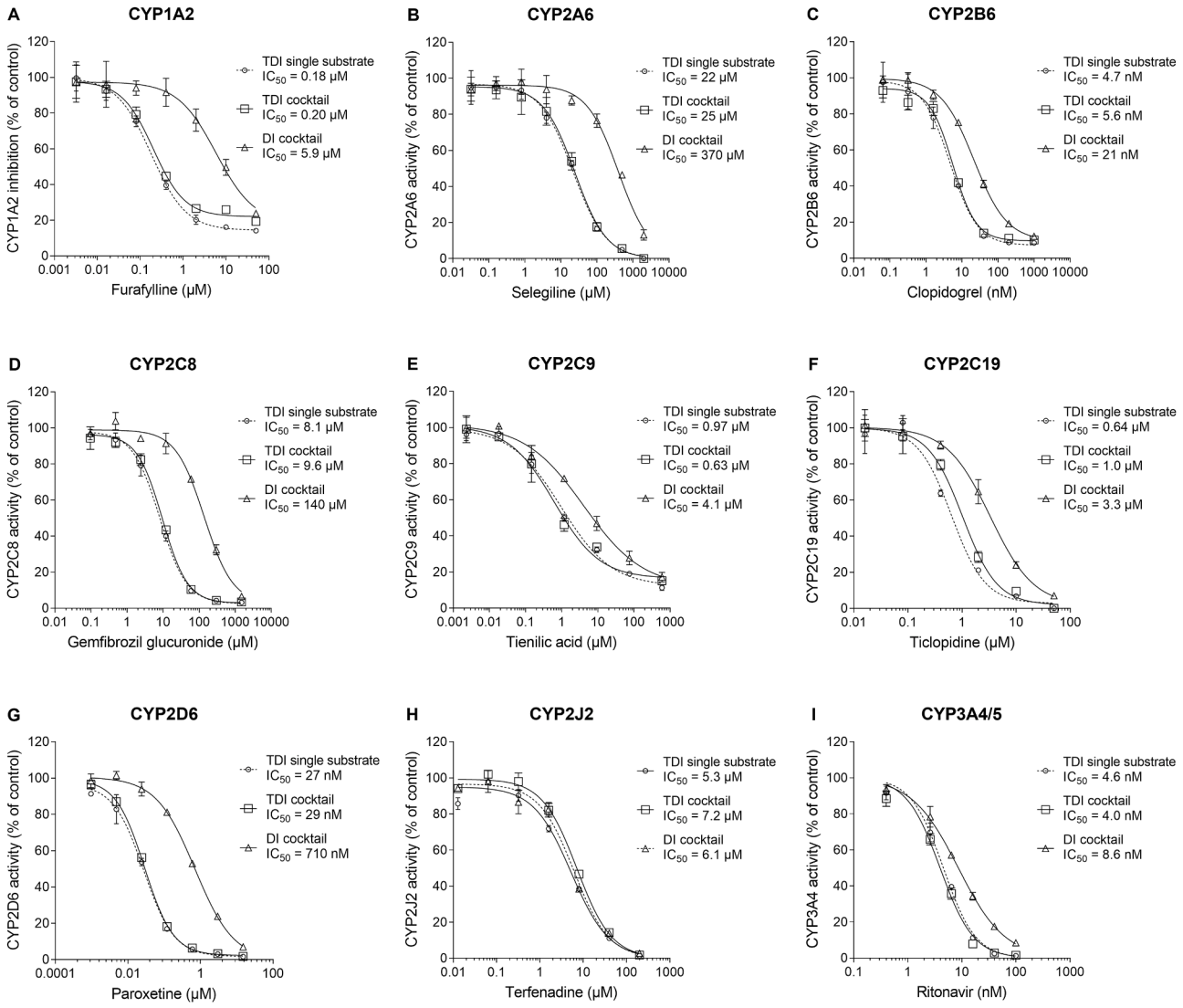

Fig. 4. The IC_{50} curves of direct inhibition (DI) and time-dependent inhibition (TDI) obtained using single substrates or the respective cocktail for each substrate in HLMs. The CYP activities are expressed as the percentage of remaining activity compared to control samples without inhibitor. Each point represents the mean ± S.D. of a single experiment run in triplicate.

less-studied CYP2J2. In the present study, we developed and validated a system comprising two fully-automated substrate cocktail methods that can be used to screen TDI of all major drug-metabolizing CYP enzymes, including CYP1A2, CYP2A6, CYP2B6, CYP2C8, CYP2C9, CYP2C19, CYP2D6, CYP2J2 and CYP3A4/5. The primary criteria considered when designing the method for TDI screening were: (1) the substrates should be selective for the chosen CYPs and the enzymatic turnover should be high enough to ensure sufficient metabolite formation; (2) inter-substrate interactions should be avoided; (3) the substrate concentrations should be near the K_m values; (4) the protein concentration should be low to avoid non-specific binding and inhibitor depletion; (5) the incubation time should be kept as short as possible to minimize time-dependent inhibition during the incubation phase and (6) the UHPLC-MS/MS sensitivity for the quantified metabolites should be good enough to detect 90% inhibition of the probe reactions. We were able to meet these requirements after several adjustments to the incubation conditions, substrate compositions and the UHPLC-MS/MS methods.

Inter-substrate interactions pose a major challenge when developing substrate cocktail methods because of the simultaneous presence of multiple substrates and metabolites and the possibility for additive effects. In particular, such interactions should be avoided when screening for mechanism-based inhibition, because competitive inhibition can hinder the inactivation process (Silverman, 1995; Ghanbari et al., 2006). Accordingly, due to multiple published interactions between the substrates (Ren et al., 2013; Spaggiari et al., 2014; Dahlinger et al., 2016), we decided to develop two separate substrate cocktails and to thoroughly scrutinize substrate-substrate interactions in the preliminary cocktails. In these experiments, the CYP2E1 substrate chlorzoxazone proved to be problematic, as it significantly inhibited both CYP1A2-mediated tacrine 1-hydroxylation and CYP2A6-mediated coumarin 7-hydroxylation. Therefore, chlorzoxazone was omitted from the cocktails. No interactions between chlorzoxazone and tacrine or coumarin have been previously reported, but these effects are consistent with the interactions of chlorzoxazone with CYP1A2-mediated caffeine metabolism and CYP2A6-mediated cotinine metabolism (Berthou et al., 1995; Nakajima et al., 1996).

Testosterone caused several interactions in cocktail I, and significantly activated CYP2E1 and had a weak inhibitory effect on CYP2C19 in cocktail II. Accordingly, to ensure sufficient CYP2C19-mediated *S*-4'-hydroxymephenytoin formation, testosterone was rejected from the cocktails. Its interactions with tolbutamide, midazolam and *S*-mephenytoin are in line with previous *in vitro* studies (Moreno-Farre et al., 2007; Zientek et al., 2008; Foti et al., 2010). Additionally, testosterone caused weak to moderate inhibition of bupropion and amodiaquine

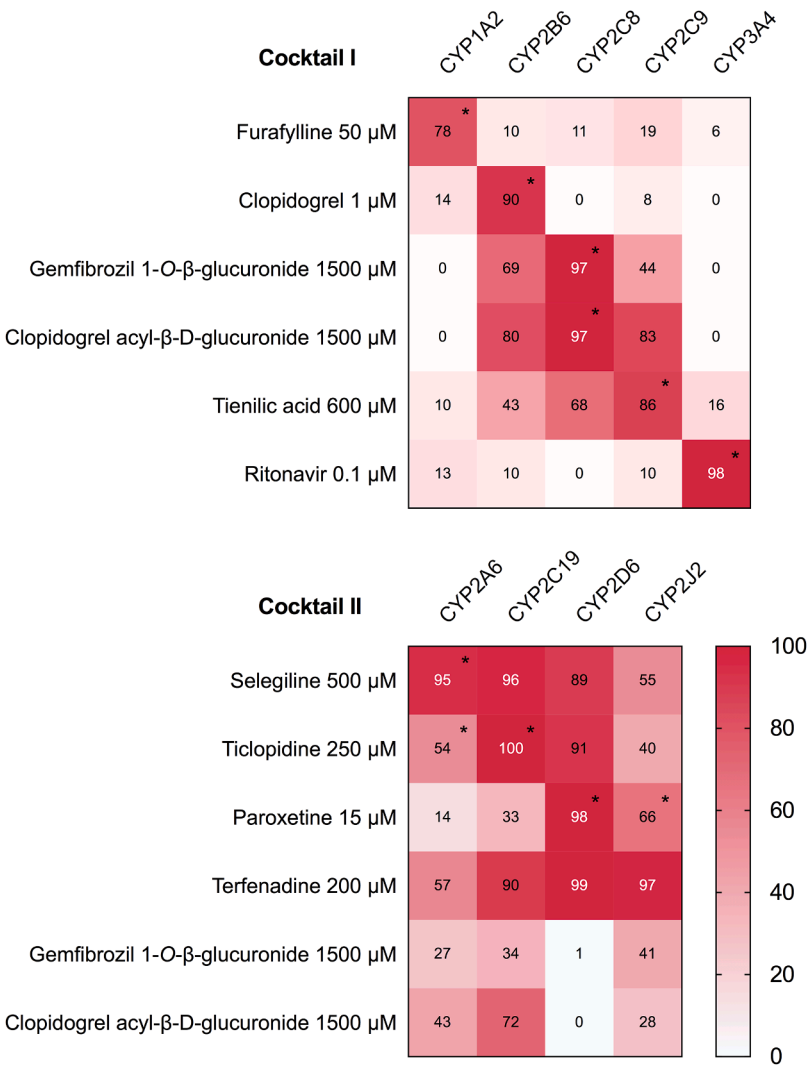

Fig. 5. Maximal inhibitory values of the reference inhibitors in IC_{50} experiments using cocktails I and II. CYP inhibition is expressed as the percentage of CYP activity inhibited without preincubation compared to solvent controls.
*, In cases where stronger inhibition was observed after a 30-minute preincubation (TDI) than without preincubation, CYP inhibition is expressed as percent inhibition with preincubation. Here, the criterion was a shift towards stronger inhibition in at least two consecutive concentration points, the shift reaching ≥15%.
All values represent the mean ± S.D. of a single experiment run in triplicate. 100% inhibition indicates that metabolite concentration was below the lower limit of quantitation.

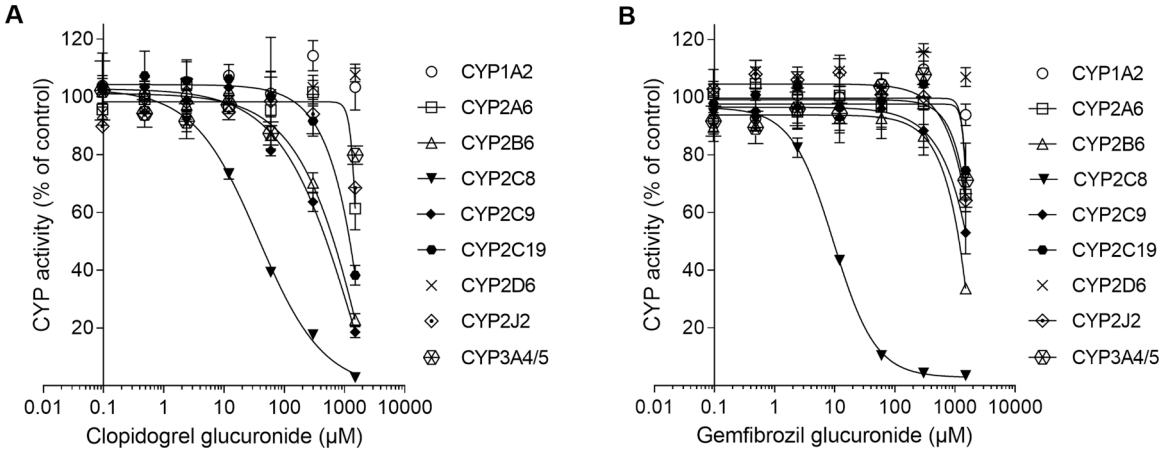

Fig. 6. The IC_{50} curves after a 30-minute preincubation with clopidogrel acyl-β–D-glucuronide (A) and gemfibrozil 1-*O*-β-glucuronide (B) in HLMs. The CYP activities are expressed as the percentage of remaining activity compared to a control sample without inhibitor. Each point represents the mean ± S.D. of a single experiment run in triplicate.

metabolism, which is in line with the contributions of CYP2B6 and CYP2C8 in testosterone metabolism (Zielinski and Mevissen, 2015). Activation of tacrine and chlorzoxazone metabolism by testosterone, on the other hand, may implicate the involvement of CYP3A4 in the metabolism of these drugs, as testosterone is known to be an allosteric effector for CYP3A4 (Gorski et al., 1997; Ueng et al., 1997; Kenworthy et al., 2001; Patki et al., 2003). Collectively, these results indicate that testosterone is not a suitable CYP3A4 substrate in cocktail systems.

Additionally, in line with previous observations (Spaggiari et al., 2014), 100 μM bupropion markedly inhibited midazolam metabolism, and bupropion concentration was thus decreased to 50 μM in the final cocktail.

K_m values for probe substrates have been rarely reported when validating substrate cocktail methods, although experimental conditions, such as the enzyme source and buffer composition, can affect enzyme kinetics (Mäenpää et al., 1998; Zhang et al., 2004; Kumar et al., 2006). The K_m values of cocktail II reactions were in the lower end of the published range of K_m values determined without BSA (Table 1). Addition of BSA in cocktail II incubations increased the rate of all probe reactions in cocktail II incubations (Supplementary Figure S3), which may have affected the K_m values. There is evidence that a small amount of BSA increases the activity of many CYP enzymes, including CYP2C19, with a decrease in K_m (Rowland et al., 2008; Peng et al., 2015; Palacharla et al., 2017). It has been suggested that the BSA effect is based on binding of free fatty acids present in microsomes, which are capable of causing competitive inhibition of CYP enzymes (Palacharla et al., 2017). Overall, the K_m values were in good accordance with previously published values, with the exception of tacrine, which exhibited biphasic kinetics (Table 1, Figure 3). The two-enzyme model gave the best fit for 1-hydroxytacrine formation, suggesting that CYP1A2 is responsible for the high affinity pathway, while another enzyme may be responsible for a low affinity, low turnover pathway. Comprehensive evaluation of the enzymes involved in tacrine metabolism is still lacking and beyond the scope of the present study, although the primary involvement of CYP1A2 in 1-hydroxytacrine formation has been well established in inhibition studies (Madden et al., 1993; Spaldin et al., 1994; Spaldin et al., 1995). Nevertheless, our results showed that 50 μM furafylline selectively and strongly (by 86%) inhibited tacrine hydroxylation, demonstrating that tacrine hydroxylation is a sensitive CYP1A2 marker reaction in the conditions used.

Omeprazole is employed sometimes as a higher turnover alternative to the CYP2C19 probe *S*-mephenytoin (Spaggiari et al., 2014). In some cocktails, it is also used as an additional CYP3A4 probe together with midazolam and testosterone (Turpeinen et al., 2005; Peng et al., 2015). However, our IC_{50} experiments using racemic omeprazole and *R*-omeprazole indicated that at 20 μM omeprazole concentration, omeprazole 5-hydroxylation is not sufficiently selective and sensitive as a CYP2C19 probe reaction *in vitro* (Supplementary Figure S1). Although CYP2C19 is the primary enzyme involved in this reaction, also other CYPs, most notably CYP3A4, are involved (Andersson et al., 1993; Karam et al., 1996; Äbelö et al., 2000).

Our final methods contain only a single probe substrate for CYP3A4, although it is often recommended that two structurally different probe substrates are used for CYP3A4 in order to take into account its multiple binding sites. Initially, testosterone and omeprazole were considered as additional CYP3A4 probes, but they were rejected from the final cocktails based on substrate interactions caused by testosterone and poor selectivity of the CYP2C19-mediated reactions of (±)-omeprazole/*R*-omeprazole described above. Substrate-dependent differences have been reported for inhibition of CYP3A4 (Galetin et al., 2005; Obach et al., 2006). However, these differences have not been prominent enough to result in false negatives when screening CYP3A4 inhibition using only midazolam, although midazolam is also a substrate of CYP3A5 (Patki et al., 2003; Galetin et al., 2005; Obach et al., 2006; Tseng et al., 2014). Moreover, the choice of the CYP3A4 probe substrate may be even less important when studying mechanism-based inhibition.

To reliably detect time-dependent inhibition, the incubation phase should be considerably shorter than the preincubation phase so that the influence of TDI taking place during the incubation could be minimized. By using sensitive UHPLC-MS/MS methods, we were able to keep the incubation time as short as 5 minutes, while keeping the protein concentration lower than in previous TDI cocktails (Atkinson et al., 2005; Mori et al., 2009; Lee, and Kim, 2013; Kozakai et al., 2014; Dahlinger et al., 2016; Chen et al., 2016). Low microsomal protein concentration minimizes the degree of non-specific binding and rapid depletion of inhibitors and substrates. A dilution method, in which preincubation of inhibitors and HLMs is conducted using 10 to 20-fold higher inhibitor and protein concentrations than those in the following incubation phase, is widely used to reduce inhibition in the incubation phase (Ghanbari et al., 2006). Yet, a high protein concentration in the preincubation phase can lead to a several-fold decrease in the extent of CYP inactivation because of non-specific binding and inhibitor depletion, as shown previously for CYP inactivation by paroxetine, ticlopidine and tienilic acid (Parkinson et al., 2011). Therefore, we chose the non-dilution method for the inhibitor screening and IC_{50} experiments, as opposed to most previously published TDI cocktail methods. However, our aim is that after identifying a time-dependent inhibitor in IC_{50} experiments, we will use an automated liquid-handling protocol to evaluate the inactivation parameters with a single substrate incubation and the dilution method.

We tested our system with well-established time-dependent inhibitors for each CYP enzyme to demonstrate its sensitivity and specificity to detect TDI in comparison to single substrate experiments (Kunze and Trager, 1993; López-Garcia et al., 1994; Koudriakova et al., 1998; Ha-Duong et al., 2001; Bertelsen et al., 2003; Richter et al., 2004; Obach et al., 2007; Siu and Tyndale, 2008; Greenblatt and Harmatz, 2015). There are no well-established time-dependent inhibitors for CYP2J2, and therefore we opted for terfenadine, which is a direct inhibitor of CYP2J2 (Matsumoto et al., 2003). As TDI was reliably detected with all time-dependent inhibitors with IC_{50} values in accordance with literature (Table 4, Figure 4) and as terfenadine caused an expected degree of direct inhibition of CYP2J2, there is no reason to doubt that TDI of CYP2J2 would not be sensitively detected with our cocktail. In addition to demonstrating the reliability of the methods, IC_{50} experiments with the reference inhibitors provided interesting insights into the CYP selectivity of the reference inhibitors. Furafylline, clopidogrel and ritonavir were highly selective inhibitors of CYP1A2, CYP2B6 and CYP3A, respectively (Figure 5). As expected, selegiline and terfenadine both inhibited CYP2C19 and CYP2D6 (Kishimoto et al., 1997; Jones et al., 1998; Nicolas et al., 1999; Taavitsainen et al., 2000; Salonen et al., 2003; Erve et al., 2013) and ticlopidine inhibited CYP2D6 in addition to their TDI target enzymes (Masimirembwa et al., 1999; Ko et al., 2000; Donato et al., 2004; Hagihara et al., 2008), providing further proof that our cocktail is suited also for detection of direct inhibition. Novel findings included TDI of CYP2A6 by ticlopidine (54% with 250 μM) and direct CYP2A6 inhibition by terfenadine (57% with 200 μM), CYP2C8 inhibition by tienilic acid (68% with 600 μM), and CYP2J2 inhibition by selegiline (55% with 500 μM). The apparent IC_{50} values were high and these inhibitory effects have therefore not been previously reported (Jean et al., 1996; Bohets et al., 2000; Flora and Tracy, 2012; Nirogi et al., 2015). However, 15 μM paroxetine inhibited CYP2J2 by 66% with preincubation and 50% without preincubation, suggesting that paroxetine is a time-dependent CYP2J2 inhibitor. This finding warrants further *in vitro* experiments.

The selectivity of CYP2C8 inhibition caused by gemfibrozil and clopidogrel glucuronides has not been studied previously in a comprehensive manner (Ogilvie et al., 2006; Tornio et al., 2014). In our experiments, it was evident that both gemfibrozil 1-O-β-glucuronide and clopidogrel acyl-β-D-glucuronide are CYP2C8-selective (Figure 6). The IC_{50} values of gemfibrozil 1-*O*-β-glucuronide and clopidogrel acyl-β-D-glucuronide were at least 100 and 10 times higher, respectively, for all other enzymes than those for CYP2C8 (9.6 and 37 μM, respectively). Particularly the CYP2C8 selectivity of gemfibrozil 1-*O*-β-glucuronide was excellent, and 50% inhibition was reached only for CYP2B6 with its highest 1500 μM concentration. Accordingly, at concentrations between 60 to 300 μM, gemfibrozil 1-*O*-β-glucuronide caused strong >90% inhibition of CYP2C8, while its inhibitory effect on other CYPs remained << 20%. Clopidogrel acyl-β-D-glucuronide, however, lost its selectivity earlier, as over 70% direct inhibition of CYP2B6, CYP2C9 and CYP2C19 was observed at 300 μM. Based on these

findings, gemfibrozil 1-*O*-β-glucuronide can be recommended as a diagnostic CYP2C8 inhibitor with 60-300 μM concentrations and a 30 min preincubation, as near complete inhibition of CYP2C8 is reached without significant effects on other CYP enzymes. Accordingly, it is clearly superior to the CYP2C8-inhibitor quercetin, which markedly inhibits also e.g. CYP1A2, CYP2C9, and CYP3A4 (Walsky et al., 2005; Rastogi and Jana, 2014; Backman et al., 2016), and better than montelukast, which slightly inhibits CYP2C9 and CYP3A4 at high concentrations and whose inhibitory effect is strongly dependent on the microsomal protein concentration used (Walsky et al., 2005). From a clinical viewpoint, it is important to note that neither gemfibrozil 1-*O*-β-glucuronide nor clopidogrel acyl-β-D-glucuronide caused time-dependent inhibition of any other CYP than CYP2C8, and their direct inhibitory effects on other CYP enzymes were weak. This indicates that these major metabolites have a low potential to cause drug interactions by inhibiting CYP enzymes, apart from CYP2C8 (Backman et al., 2016; Itkonen et al., 2019).

The automated incubation method provides many advantages over manual experiments, which are particularly useful in screening experiments requiring high throughput. In addition to increasing the efficiency of the whole process, beginning from the automated incubations in 96-well plates and ending to concentration measurements, automated liquid handling methods reduce the possibility of errors and provide a high level of reproducibility, as demonstrated by the low variability observed in our experiments. Automation also considerably reduces the amount of manual work requiring precision, attentiveness and repetitive movements, thus mitigating ergonomical concerns. A disadvantage of automation is the laborious planning of the experimental process and creation of programming scripts, including intricate timings and adaptation of liquid classes to ensure precise pipetting volumes for different matrices and liquids. Therefore, automation cannot be recommended for simple and infrequently repeated protocols. However, if large-scale screening or complex experiments requiring frequent pipetting and precision are planned, automation has significant advantages over manual work. To enable easier implementation of automation, we will share detailed instructions concerning our system and its updates on a data repository (DOI: 10.5281/zenodo.4554651).

In conclusion, we optimized and validated two substrate cocktail methods for fully automated screening of both direct and time-dependent inhibition of nine major CYP enzymes, including the less studied CYP2J2. Improvements compared to previous TDI cocktail methods include automation, a short incubation time, a low protein concentration in both preincubation and incubation phases and a thorough validation, including assessment of possible substrate interactions. No significant interactions between the substrates in the final cocktails were observed and the IC_{50} values of the reference inhibitors in cocktails were comparable to those obtained using single substrates. The cocktail methods not only enhance the throughput of TDI screening but also allow simultaneous investigation of the selectivity of time-dependent CYP inhibition. Gemfibrozil 1-*O*-β-glucuronide was found to be a selective time-dependent inhibitor of CYP2C8, with no significant inhibitory effect on other major CYP enzymes at concentrations up to 300 μM. The findings imply that gemfibrozil 1-*O*-β-glucuronide can be used as a strong and selective inhibitor of CYP2C8 in *in vitro* studies aimed to estimate the roles of individual CYPs in the metabolism of an investigational drug.

Author contributions

Helinä Kahma: Methodology, Investigation, Formal analysis, Validation, Visualization, Writing – Original Draft, Writing – Review & Editing

Laura Aurinsalo: Methodology, Investigation, Formal analysis, Validation, Visualization, Writing – Original Draft, Writing – Review & Editing

Mikko Neuvonen: Methodology, Writing – Review & Editing

Jani Katajamäki: Methodology, Investigation, Formal analysis

Marie-Noëlle Paludetto: Investigation, Formal analysis

Jenni Viinamäki: Methodology

Terhi Launiainen: Methodology

Anne M. Filppula: Investigation, Writing – Review & Editing

Aleksi Tornio: Writing – Review & Editing, Supervision

Mikko Niemi: Writing – Review & Editing, Supervision, Funding acquisition

Janne T. Backman: Conceptualization, Writing – Review & Editing, Supervision, Funding acquisition, Project administration

Declaration of competing interest

None.

Acknowledgments

This study has been financially supported by grants from the Academy of Finland [Grant decisions 278123, 2014 and 325667, 2019] (Helsinki, Finland), Sigrid Jusélius Foundation [Grant number 8037] (Helsinki, Finland), the Finnish Cultural Foundation [Grant decision 190434, 2019] (Helsinki, Finland), and by State funding for university-level health research (Hospital District of Helsinki and Uusimaa, Finland).

Supplementary materials

Supplementary material associated with this article can be found, in the online version, at doi:10.1016/j.ejps.2021.105810.

References

World Health Organization, 2001. Voluntary withdrawal of Cerivastatin – Reports of Rhabdomyolysis. https://www.who.int/medicines/publications/drugalerts/DrugAlert102.pdf?ua=1 (accessed 2020-06-11).

European Medicines Agency, 2012. Guideline on the investigation of drug interactions. https://www.ema.europa.eu/en/documents/scientific-guideline/guideline-investigation-drug-interactions-revision-1_en.pdf (accessed 2020-06-11) .

U.S. Food and Drug Administration, 2020. In Vitro Drug Interaction Studies – Cytochrome P450 Enzyme- and Transporter-Mediated Drug Interactions Guidance for Industry. https://www.fda.gov/media/134582/download (accessed 2020-06-11) .

Äbelö, A., Andersson, T.B., Antonsson, M., Naudot, A.K., Skånberg, I., Weidolf, L., 2000. Stereoselective metabolism of omeprazole by human cytochrome P450 enzymes. Drug Metab. Dispos. 28, 966–972.

Andersson, T., Miners, J.O., Veronese, M.E., Tassaneeyakul, W., Tassaneeyakul, W., Meyer, U.A., Birkett, D.J., 1993. Identification of human liver cytochrome P450 isoforms mediating omeprazole metabolism. Br. J. Clin. Pharmacol. 36, 521–530.

Atkinson, A., Kenny, J.R., Grime, K., 2005. Automated assessment of time-dependent inhibition of human cytochrome P450 enzymes using liquid chromatography-tandem mass spectrometry analysis. Drug Metab. Dispos. 33, 1637–1647.

Backman, J.T., Kyrklund, C., Neuvonen, M., Neuvonen, P.J., 2002. Gemfibrozil greatly increases plasma concentrations of cerivastatin. Clin. Pharmacol. Ther. 72, 685–691.

Backman, J.T., Honkalammi, J., Neuvonen, M., Kurkinen, K.J., Tornio, A., Niemi, M., Neuvonen, P.J., 2009. CYP2C8 activity recovers within 96 hours after gemfibrozil dosing: estimation of CYP2C8 half-life using repaglinide as an in vivo probe. Drug Metab. Dispos. 37, 2359–2366.

Backman, J.T., Filppula, A.M., Niemi, M., Neuvonen, P.J., 2016. Role of Cytochrome P450 2C8 in Drug Metabolism and Interactions. Pharmacol. Rev. 68, 168–241.

Bertelsen, K.M., Venkatakrishnan, K., Von Moltke, L.L., Obach, R.S., Greenblatt, D.J., 2003. Apparent mechanism-based inhibition of human CYP2D6 in vitro by paroxetine: comparison with fluoxetine and quinidine. Drug Metab. Dispos. 31, 289–293.

Berthou, F., Goasduff, T., Lucas, D., Dréano, Y., Le Bot, M.H., Ménez, J.F., 1995. Interaction between two probes used for phenotyping cytochromes P4501A2 (caffeine) and P4502E1 (chlorzoxazone) in humans. Pharmacogenetics 5, 72–79.

Bohets, H., Lavrijsen, K., Hendrickx, J., van Houdt, J., van Genechten, V., Verboven, P., Meuldermans, W., Heykants, J., 2000. Identification of the cytochrome P450 enzymes involved in the metabolism of cisapride: in vitro studies of potential co-medication interactions. Br. J. Pharmacol. 129, 1655–1667.

Chen, Z.H., Zhang, S.X., Long, N., Lin, L.S., Chen, T., Zhang, F.P., Lv, X.Q., Ye, P.Z., Li, N., Zhang, K.Z., 2016. An improved substrate cocktail for assessing direct inhibition and time-dependent inhibition of multiple cytochrome P450s. Acta Pharmacol. Sin. 37, 708–718.

Cohen, L.H., Remley, M.J., Raunig, D., Vaz, A.D., 2003. In vitro drug interactions of cytochrome p450: an evaluation of fluorogenic to conventional substrates. Drug Metab. Dispos. 31, 1005–1015.
Dahlinger, D., Duechting, S., Nuecken, D., Sydow, K., Fuhr, U., Frechen, S., 2016. Development and validation of an in vitro, seven-in-one human cytochrome P450 assay for evaluation of both direct and time-dependent inhibition. J. Pharmacol. Toxicol. Methods 77, 66–75.
Donato, M.T., Jiménez, N., Castell, J.V., Gómez-Lechón, M.J., 2004. Fluorescence-based assays for screening nine cytochrome P450 (P450) activities in intact cells expressing individual human P450 enzymes. Drug Metab. Dispos. 32, 699–706.
Erve, J.C., Gauby, S., Maynard Jr., J.W., Svensson, M.A., Tonn, G., Quinn, K.P., 2013. Bioactivation of sitaxentan in liver microsomes, hepatocytes, and expressed human P450s with characterization of the glutathione conjugate by liquid chromatography tandem mass spectrometry. Chem. Res. Toxicol. 26, 926–936.
Flora, D.R., Tracy, T.S., 2012. Development of an in vitro system with human liver microsomes for phenotyping of CYP2C9 genetic polymorphisms with a mechanism-based inactivator. Drug Metab. Dispos. 40, 836–842.
Floyd, J.S., Kaspera, R., Marciante, K.D., Weiss, N.S., Heckbert, S.R., Lumley, T., Wiggins, K.L., Tamraz, B., Kwok, P.Y., Totah, R.A., Psaty, B.M., 2012. A screening study of drug-drug interactions in cerivastatin users: an adverse effect of clopidogrel. Clin. Pharmacol. Ther. 91, 896–904.
Foti, R.S., Rock, D.A., Wienkers, L.C., Wahlstrom, J.L., 2010. Selection of alternative CYP3A4 probe substrates for clinical drug interaction studies using in vitro data and in vivo simulation. Drug Metab. Dispos. 38, 981–987.
Galetin, A., Ito, K., Hallifax, D., Houston, J.B., 2005. CYP3A4 substrate selection and substitution in the prediction of potential drug-drug interactions. J. Pharmacol. Exp. Ther. 314, 180–190.
Ghanbari, F., Rowland-Yeo, K., Bloomer, J.C., Clarke, S.E., Lennard, M.S., Tucker, G.T., Rostami-Hodjegan, A., 2006. A critical evaluation of the experimental design of studies of mechanism based enzyme inhibition, with implications for in vitro-in vivo extrapolation. Curr. Drug Metab. 7, 315–334.
Gorski, J.C., Jones, D.R., Wrighton, S.A., Hall, S.D., 1997. Contribution of human CYP3A subfamily members to the 6-hydroxylation of chlorzoxazone. Xenobiotica 27, 243–256.
Greenblatt, D.J., Harmatz, J.S., 2015. Ritonavir is the best alternative to ketoconazole as an index inhibitor of cytochrome P450-3A in drug-drug interaction studies. Br. J. Clin. Pharmacol. 80, 342–350.
Guengerich, F.P., 2003. Cytochrome P450 oxidations in the generation of reactive electrophiles: epoxidation and related reactions. Arch. Biochem. Biophys. 409, 59–71.
Ha-Duong, N.T., Dijols, S., Macherey, A.C., Goldstein, J.A., Dansette, P.M., Mansuy, D., 2001. Ticlopidine as a selective mechanism-based inhibitor of human cytochrome P450 2C19. Biochemistry 40, 12112–12122.
Hagihara, K., Nishiya, Y., Kurihara, A., Kazui, M., Farid, N.A., Ikeda, T., 2008. Comparison of human cytochrome P450 inhibition by the thienopyridines prasugrel, clopidogrel, and ticlopidine. Drug Metab. Pharmacokinet. 23, 412–420.
Hashizume, T., Imaoka, S., Mise, M., Terauchi, Y., Fujii, T., Miyazaki, H., Kamataki, T., Funae, Y., 2002. Involvement of CYP2J2 and CYP4F12 in the metabolism of ebastine in human intestinal microsomes. J. Pharmacol. Exp. Ther. 300, 298–304.
Honkalammi, J., Niemi, M., Neuvonen, P.J., Backman, J.T., 2011a. Dose-dependent interaction between gemfibrozil and repaglinide in humans: strong inhibition of CYP2C8 with subtherapeutic gemfibrozil doses. Drug Metab. Dispos. 39, 1977–1986.
Honkalammi, J., Niemi, M., Neuvonen, P.J., Backman, J.T., 2011b. Mechanism-based inactivation of CYP2C8 by gemfibrozil occurs rapidly in humans. Clin. Pharmacol. Ther. 89, 579–586.
Honkalammi, J., Niemi, M., Neuvonen, P.J., Backman, J.T., 2012. Gemfibrozil is a strong inactivator of CYP2C8 in very small multiple doses. Clin. Pharmacol. Ther. 91, 846–855.
Itkonen, M.K., Tornio, A., Neuvonen, M., Neuvonen, P.J., Niemi, M., Backman, J.T., 2019. Clopidogrel and gemfibrozil strongly inhibit the CYP2C8-dependent formation of 3-hydroxydesloratadine and increase desloratadine exposure in humans. Drug Metab. Dispos. 47, 377–385.
Jean, P., Lopez-Garcia, P., Dansette, P., Mansuy, D., Goldstein, J.L., 1996. Oxidation of tienilic acid by human yeast-expressed cytochromes P-450 2C8, 2C9, 2C18 and 2C19. Evidence that this drug is a mechanism-based inhibitor specific for cytochrome P-450 2C9. Eur. J. Biochem. 241, 797–804.
Jones, B.C., Hyland, R., Ackland, M., Tyman, C.A., Smith, D.A., 1998. Interaction of terfenadine and its primary metabolites with cytochrome P450 2D6. Drug Metab. Dispos. 26, 875–882.
Juřica, J., Žourková, A., 2013. Dynamics and persistence of CYP2D6 inhibition by paroxetine. J. Clin. Pharm. Ther. 38, 294–300.
Kaartinen, T.J.K., Tornio, A., Tapaninen, T., Launiainen, T., Isoherranen, N., Niemi, M., Backman, J.T., 2020. Effect of High-Dose Esomeprazole on CYP1A2, CYP2C19, and CYP3A4 Activities in Humans: Evidence for Substantial and Long-lasting Inhibition of CYP2C19. Clin. Pharmacol. Ther. 108, 1254–1264.
Kahma, H., Filppula, A.M., Launiainen, T., Viinamäki, J., Neuvonen, M., Evangelista, E. A., Totah, R.A., Backman, J.T., 2019. Critical Differences between Enzyme Sources in Sensitivity to Detect Time-Dependent Inactivation of CYP2C8. Drug Metab. Dispos. 47, 436–443.
Kalgutkar, A.S., Obach, R.S., Maurer, T.S., 2007. Mechanism-based inactivation of cytochrome P450 enzymes: chemical mechanisms, structure-activity relationships and relationship to clinical drug-drug interactions and idiosyncratic adverse drug reactions. Curr. Drug Metab. 8, 407–447.
Karam, W.G., Goldstein, J.A., Lasker, J.M., Ghanayem, B.I., 1996. Human CYP2C19 is a major omeprazole 5-hydroxylase, as demonstrated with recombinant cytochrome P450 enzymes. Drug Metab. Dispos. 24, 1081–1087.
Karkhanis, A., Hong, Y., Chan, E.C.Y., 2017. Inhibition and inactivation of human CYP2J2: Implications in cardiac pathophysiology and opportunities in cancer therapy. Biochem. Pharmacol. 135, 12–21.
Kenworthy, K.E., Clarke, S.E., Andrews, J., Houston, J.B., 2001. Multisite kinetic models for CYP3A4: simultaneous activation and inhibition of diazepam and testosterone metabolism. Drug Metab. Dispos. 29, 1644–1651.
Kishimoto, W., Hiroi, T., Sakai, K., Funae, Y., Igarashi, T., 1997. Metabolism of epinastine, a histamine H1 receptor antagonist, in human liver microsomes in comparison with that of terfenadine. Res. Commun. Mol. Pathol. Pharmacol. 98, 273–292.
Ko, J.W., Desta, Z., Soukhova, N.V., Tracy, T., Flockhart, D.A., 2000. In vitro inhibition of the cytochrome P450 (CYP450) system by the antiplatelet drug ticlopidine: potent effect on CYP2C19 and CYP2D6. Br. J. Clin. Pharmacol. 49, 343–351.
Koudriakova, T., Iatsimirskaia, E., Utkin, I., Gangl, E., Vouros, P., Storozhuk, E., Orza, D., Marinina, J., Gerber, N., 1998. Metabolism of the human immunodeficiency virus protease inhibitors indinavir and ritonavir by human intestinal microsomes and expressed cytochrome P4503A4/3A5: mechanism-based inactivation of cytochrome P4503A by ritonavir. Drug Metab. Dispos. 26, 552–561.
Kozakai, K., Yamada, Y., Oshikata, M., Kawase, T., Suzuki, E., Haramaki, Y., Taniguchi, H., 2014. Cocktail-substrate approach-based high-throughput assay for evaluation of direct and time-dependent inhibition of multiple cytochrome P450 isoforms. Drug Metab. Pharmacokinet. 29, 198–207.
Kumar, V., Rock, D.A., Warren, C.J., Tracy, T.S., Wahlstrom, J.L., 2006. Enzyme source effects on CYP2C9 kinetics and inhibition. Drug Metab. Dispos. 34, 1903–1908.
Kunze, K.L., Trager, W.F., 1993. Isoform-selective mechanism-based inhibition of human cytochrome P450 1A2 by furafylline. Chem. Res. Toxicol. 6, 649–656.
Lee, C.A., Neul, D., Clouser-Roche, A., Dalvie, D., Wester, M.R., Jiang, Y., Jones 3rd, J.P., Freiwald, S., Zientek, M., Totah, R.A., 2010. Identification of novel substrates for human cytochrome P450 2J2. Drug Metab. Dispos. 38, 347–356.
Lee, K.S., Kim, S.K., 2013. Direct and metabolism-dependent cytochrome P450 inhibition assays for evaluating drug-drug interactions. J. Appl. Toxicol. 33, 100–108.
López-Garcia, M.P., Dansette, P.M., Mansuy, D., 1994. Thiophene derivatives as new mechanism-based inhibitors of cytochromes P-450: inactivation of yeast-expressed human liver cytochrome P-450 2C9 by tienilic acid. Biochemistry 33, 166–175.
Madden, S., Woolf, T.F., Pool, W.F., Park, B.K., 1993. An investigation into the formation of stable, protein-reactive and cytotoxic metabolites from tacrine in vitro. Studies with human and rat liver microsomes. Biochem. Pharmacol. 46, 13–20.
Mäenpää, J., Hall, S.D., Ring, B.J., Strom, S.C., Wrighton, S.A., 1998. Human cytochrome P450 3A (CYP3A) mediated midazolam metabolism: the effect of assay conditions and regioselective stimulation by alpha-naphthoflavone, terfenadine and testosterone. Pharmacogenetics 8, 137–155.
Masimirembwa, C.M., Otter, C., Berg, M., Jönsson, M., Leidvik, B., Jonsson, E., Johansson, T., Bäckman, A., Edlund, A., Andersson, T.B., 1999. Heterologous expression and kinetic characterization of human cytochromes P-450: validation of a pharmaceutical tool for drug metabolism research. Drug Metab. Dispos. 27, 1117–1122.
Matsumoto, S., Hirama, T., Kim, H.J., Nagata, K., Yamazoe, Y., 2003. In vitro inhibition of human small intestinal and liver microsomal astemizole O-demethylation: different contribution of CYP2J2 in the small intestine and liver. Xenobiotica 33, 615–623.
Moreno-Farre, J., Workman, P., Raynaud, F., 2007. Analysis of potential drug–drug interactions for anticancer agents in human liver microsomes by high throughput liquid chromatography/mass spectrometry assay. Aust. J. Cancer 6, 55–69.
Mori, K., Hashimoto, H., Takatsu, H., Tsuda-Tsukimoto, M., Kume, T., 2009. Cocktail-substrate assay system for mechanism-based inhibition of CYP2C9, CYP2D6, and CYP3A using human liver microsomes at an early stage of drug development. Xenobiotica 39, 415–422.
Nakajima, M., Yamamoto, T., Nunoya, K., Yokoi, T., Nagashima, K., Inoue, K., Funae, Y., Shimada, N., Kamataki, T., Kuroiwa, Y., 1996. Characterization of CYP2A6 involved in 3′-hydroxylation of cotinine in human liver microsomes. J. Pharmacol. Exp. Ther. 277, 1010–1015.
Nicolas, J.M., Whomsley, R., Collart, P., Roba, J., 1999. In vitro inhibition of human liver drug metabolizing enzymes by second generation antihistamines. Chem. Biol. Interact. 123, 63–79.
Nirogi, R., Palacharla, R.C., Uthukam, V., Manoharan, A., Srikakolapu, S.R., Kalaikadhiban, I., Boggavarapu, R.K., Ponnamaneni, R.K., Ajjala, D.R., Bhyrapuneni, G., 2015. Chemical inhibitors of CYP450 enzymes in liver microsomes: combining selectivity and unbound fractions to guide selection of appropriate concentration in phenotyping assays. Xenobiotica 45, 95–106.
Obach, R.S., Walsky, R.L., Venkatakrishnan, K., Gaman, E.A., Houston, J.B., Tremaine, L. M., 2006. The utility of in vitro cytochrome P450 inhibition data in the prediction of drug-drug interactions. J. Pharmacol. Exp. Ther. 316, 336–348.
Obach, R.S., Walsky, R.L., Venkatakrishnan, K., 2007. Mechanism-based inactivation of human cytochrome p450 enzymes and the prediction of drug-drug interactions. Drug Metab. Dispos. 35, 246–255.
Ogilvie, B.W., Zhang, D., Li, W., Rodrigues, A.D., Gipson, A.E., Holsapple, J., Toren, P., Parkinson, A., 2006. Glucuronidation converts gemfibrozil to a potent, metabolism-dependent inhibitor of CYP2C8: implications for drug-drug interactions. Drug Metab. Dispos. 34, 191–197.
Palacharla, R.C., Uthukam, V., Manoharan, A., Ponnamaneni, R.K., Padala, N.P., Boggavarapu, R.K., Bhyrapuneni, G., Ajjala, D.R., Nirogi, R., 2017. Inhibition of cytochrome P450 enzymes by saturated and unsaturated fatty acids in human liver microsomes, characterization of enzyme kinetics in the presence of bovine serum albumin (0.1 and 1.0% w/v) and in vitro - in vivo extrapolation of hepatic clearance. Eur. J. Pharm. Sci. 101, 80–89.

Parkinson, A., Kazmi, F., Buckley, D.B., Yerino, P., Ogilvie, B.W., Paris, B.L., 2010. System-dependent outcomes during the evaluation of drug candidates as inhibitors of cytochrome P450 (CYP) and uridine diphosphate glucuronosyltransferase (UGT) enzymes: human hepatocytes versus liver microsomes versus recombinant enzymes. Drug Metab. Pharmacokinet. 25, 16–27.

Parkinson, A., Kazmi, F., Buckley, D.B., Yerino, P., Paris, B.L., Holsapple, J., Toren, P., Otradovec, S.M., Ogilvie, B.W., 2011. An evaluation of the dilution method for identifying metabolism-dependent inhibitors of cytochrome P450 enzymes. Drug Metab. Dispos. 39, 1370–1387.

Patki, K.C., Von Moltke, L.L., Greenblatt, D.J., 2003. In vitro metabolism of midazolam, triazolam, nifedipine, and testosterone by human liver microsomes and recombinant cytochromes p450: role of cyp3a4 and cyp3a5. Drug Metab. Dispos. 31, 938–944.

Peng, Y., Wu, H., Zhang, X., Zhang, F., Qi, H., Zhong, Y., Wang, Y., Sang, H., Wang, G., Sun, J., 2015. A comprehensive assay for nine major cytochrome P450 enzymes activities with 16 probe reactions on human liver microsomes by a single LC/MS/MS run to support reliable in vitro inhibitory drug-drug interaction evaluation. Xenobiotica 45, 961–977.

Rastogi, H., Jana, S., 2014. Evaluation of inhibitory effects of caffeic acid and quercetin on human liver cytochrome p450 activities. Phytother. Res. 28, 1873–1878.

Ren, S., Zeng, J., Mei, Y., Zhang, J.Z., Yan, S.F., Fei, J., Chen, L., 2013. Discovery and characterization of novel, potent, and selective cytochrome P450 2J2 inhibitors. Drug Metab. Dispos. 41, 60–71.

Richter, T., Mürdter, T.E., Heinkele, G., Pleiss, J., Tatzel, S., Schwab, M., Eichelbaum, M., Zanger, U.M., 2004. Potent mechanism-based inhibition of human CYP2B6 by clopidogrel and ticlopidine. J. Pharmacol. Exp. Ther. 308, 189–197.

Roca, B., Calvo, B., Monferrer, R., 2002. Severe rhabdomyolysis and cerivastatin-gemfibrozil combination therapy. Ann. Pharmacother. 36, 730–731.

Rowland, A., Elliot, D.J., Knights, K.M., Mackenzie, P.I., Miners, J.O., 2008. The "albumin effect" and in vitro-in vivo extrapolation: sequestration of long-chain unsaturated fatty acids enhances phenytoin hydroxylation by human liver microsomal and recombinant cytochrome P450 2C9. Drug Metab. Dispos. 36, 870–877.

Sadeque, A.J., Fisher, M.B., Korzekwa, K.R., Gonzalez, F.J., Rettie, A.E., 1997. Human CYP2C9 and CYP2A6 mediate formation of the hepatotoxin 4-ene-valproic acid. J. Pharmacol. Exp. Ther. 283, 698–703.

Salonen, J.S., Nyman, L., Boobis, A.R., Edwards, R.J., Watts, P., Lake, B.G., Price, R.J., Renwick, A.B., Gómez-Lechón, M.J., Castell, J.V., Ingelman-Sundberg, M., Hidestrand, M., Guillouzo, A., Corcos, L., Goldfarb, P.S., Lewis, D.F., Taavitsainen, P., Pelkonen, O., 2003. Comparative studies on the cytochrome p450-associated metabolism and interaction potential of selegiline between human liver-derived in vitro systems. Drug Metab. Dispos. 31, 1093–1102.

Silverman, R.B., 1995. Mechanism-based enzyme inactivators. Methods Enzymol 249, 240–283.

Siu, E.C., Tyndale, R.F., 2008. Selegiline is a mechanism-based inactivator of CYP2A6 inhibiting nicotine metabolism in humans and mice. J. Pharmacol. Exp. Ther. 324, 992–999.

Spaggiari, D., Geiser, L., Daali, Y., Rudaz, S., 2014. A cocktail approach for assessing the in vitro activity of human cytochrome P450s: an overview of current methodologies. J. Pharm. Biomed. Anal. 101, 221–237.

Spaldin, V., Madden, S., Pool, W.F., Woolf, T.F., Park, B.K., 1994. The effect of enzyme inhibition on the metabolism and activation of tacrine by human liver microsomes. Br. J. Clin. Pharmacol. 38, 15–22.

Spaldin, V., Madden, S., Adams, D.A., Edwards, R.J., Davies, D.S., Park, B.K., 1995. Determination of human hepatic cytochrome P4501A2 activity in vitro use of tacrine as an isoenzyme-specific probe. Drug Metab. Dispos. 23, 929–934.

Spracklin, D.K., Thummel, K.E., Kharasch, E.D., 1996. Human reductive halothane metabolism in vitro is catalyzed by cytochrome P450 2A6 and 3A4. Drug Metab. Dispos. 24, 976–983.

Taavitsainen, P., Anttila, M., Nyman, L., Karnani, H., Salonen, J.S., Pelkonen, O., 2000. Selegiline metabolism and cytochrome P450 enzymes: in vitro study in human liver microsomes. Pharmacol. Toxicol. 86, 215–221.

Thompson, P.D., Clarkson, P., Karas, R.H., 2003. Statin-associated myopathy. JAMA 289, 1681–1690.

Tornio, A., Niemi, M., Neuvonen, M., Laitila, J., Kalliokoski, A., Neuvonen, P.J., Backman, J.T., 2008. The effect of gemfibrozil on repaglinide pharmacokinetics persists for at least 12 h after the dose: evidence for mechanism-based inhibition of CYP2C8 in vivo. Clin. Pharmacol. Ther. 84, 403–411.

Tornio, A., Filppula, A.M., Kailari, O., Neuvonen, M., Nyrönen, T.H., Tapaninen, T., Neuvonen, P.J., Niemi, M., Backman, J.T., 2014. Glucuronidation converts clopidogrel to a strong time-dependent inhibitor of CYP2C8: a phase II metabolite as a perpetrator of drug-drug interactions. Clin. Pharmacol. Ther. 96, 498–507.

Tornio, A., Neuvonen, P.J., Niemi, M., Backman, J.T., 2017. Role of gemfibrozil as an inhibitor of CYP2C8 and membrane transporters. Expert Opin. Drug Metab. Toxicol. 13, 83–95.

Tseng, E., Walsky, R.L., Luzietti Jr., R.A., Harris, J.J., Kosa, R.E., Goosen, T.C., Zientek, M.A., Obach, R.S., 2014. Relative contributions of cytochrome CYP3A4 versus CYP3A5 for CYP3A-cleared drugs assessed in vitro using a CYP3A4-selective inactivator (CYP3cide). Drug Metab. Dispos. 42, 1163–1173.

Turpeinen, M., Uusitalo, J., Jalonen, J., Pelkonen, O., 2005. Multiple P450 substrates in a single run: rapid and comprehensive in vitro interaction assay. Eur. J. Pharm. Sci. 24, 123–132.

Ueng, Y.F., Kuwabara, T., Chun, Y.J., Guengerich, F.P., 1997. Cooperativity in oxidations catalyzed by cytochrome P450 3A4. Biochemistry 36, 370–381.

Walsky, R.L., Obach, R.S., Gaman, E.A., Gleeson, J.P., Proctor, W.R., 2005. Selective inhibition of human cytochrome P4502C8 by montelukast. Drug Metab. Dispos. 33, 413–418.

Zhang, Z., Li, Y., Shou, M., Zhang, Y., Ngui, J.S., Stearns, R.A., Evans, D.C., Baillie, T.A., Tang, W., 2004. Influence of different recombinant systems on the cooperativity exhibited by cytochrome P4503A4. Xenobiotica 34, 473–486.

Zielinski, J., Mevissen, M., 2015. Inhibition of in vitro metabolism of testosterone in human, dog and horse liver microsomes to investigate species differences. Toxicol. In. Vitro. 29, 468–478.

Zientek, M., Miller, H., Smith, D., Dunklee, M.B., Heinle, L., Thurston, A., Lee, C., Hyland, R., Fahmi, O., Burdette, D., 2008. Development of an in vitro drug-drug interaction assay to simultaneously monitor five cytochrome P450 isoforms and performance assessment using drug library compounds. J. Pharmacol. Toxicol. Methods 58, 206–214.